Applied Numerical Mathematics 113 (2017) 71–92

Contents lists available at ScienceDirect

Applied Numerical Mathematics

www.elsevier.com/locate/apnum

Highly stable implicit–explicit Runge–Kutta methods

Giuseppe Izzo [a,*,1], Zdzislaw Jackiewicz [b,c]

[a] Dipartimento di Matematica e Applicazioni "R.Caccioppoli", Università di Napoli "Federico II", 80126 Napoli, Italy
[b] Department of Mathematics, Arizona State University, Tempe, AZ 85287, United States
[c] AGH University of Science and Technology, Kraków, Poland

ARTICLE INFO

Article history:
Received 1 August 2016
Accepted 25 October 2016
Available online 15 November 2016

Keywords:
Runge–Kutta methods
Implicit–explicit methods
Stability analysis
Strong stability preserving
Courant–Friedrichs–Levy condition
Hyperbolic conservation laws

ABSTRACT

We investigate implicit–explicit (IMEX) Runge–Kutta (RK) methods for differential systems with non-stiff and stiff processes. The construction of such methods with large regions of absolute stability of the 'explicit part' of the method assuming that the 'implicit part' of the scheme is A-stable, is described. We also describe the construction of IMEX RK methods, where the 'explicit part' of the schemes have strong stability properties. Examples of highly stable IMEX RK methods are provided up to the order $p = 4$. Numerical examples are also given which illustrate good performance of these schemes.

1. Introduction

Consider the initial-value problem for a system of ordinary differential equations (ODEs) of the form

$$\begin{cases} y'(t) = f\big(y(t)\big) + g\big(y(t)\big), \quad t \in [t_0, T], \\ y(t_0) = y_0, \end{cases} \tag{1.1}$$

where the functions $f : \mathbb{R}^m \to \mathbb{R}^m$ and $g : \mathbb{R}^m \to \mathbb{R}^m$ are assumed to be sufficiently smooth. In many practical applications the terms $f(y)$ and $g(y)$ represent processes evolving on different time scales. For example $f(y)$ may correspond to the non-stiff and $g(y)$ to the stiff processes. Such systems may arise from the semi-discretization in space variables of time dependent partial differential equations (PDEs) such as, for example, advection–diffusion–reaction equations, or hyperbolic conservation laws with relaxation. The advection–diffusion–reaction equation in one space variable x takes the form

$$\frac{\partial y}{\partial t} + \frac{\partial (ay)}{\partial x} = \frac{\partial}{\partial x}\left(d\,\frac{\partial y}{\partial x}\right) + r(y), \quad x \in [a, b], \quad t \in [t_0, T], \tag{1.2}$$

where the advection and diffusion coefficients $a = a(x, t)$ and $d = d(x, t)$ may depend on x and t but are independent of the concentration y, and the term $r(y)$ corresponds to sources, sinks, and chemical reactions. Discretization of the equation (1.2) in space variable x, with appropriate boundary and initial conditions, leads to the system of the form (1.1) with $f(y)$ corresponding to the discretization of the term $-\partial(ay)/\partial x$, and $g(y)$ corresponding to the discretization of the term $\partial(d\,\partial y/\partial x)/\partial x + r(y)$. In one space dimension an example of a hyperbolic system with relaxation takes the form

* Corresponding author.
E-mail addresses: giuseppe.izzo@unina.it (G. Izzo), jackiewicz@asu.edu (Z. Jackiewicz).

[1] The work of this author was partially supported by INdAM-GNCS.

http://dx.doi.org/10.1016/j.apnum.2016.10.018
0168-9274/

$$\frac{\partial y}{\partial t} + \frac{\partial F(y)}{\partial x} = \frac{1}{\epsilon} R(y), \quad x \in [a,b], \quad t \in [t_0, T], \tag{1.3}$$

which takes the form (1.1) with $f(y)$ corresponding to the discretization of $-\partial F(y)/\partial x$, and with $g(y)$ corresponding to $R(y)/\epsilon$.

We will discretize the non-stiff part of (1.1) by an explicit integration formula and the stiff part of (1.1) by an implicit method. This leads to the class of so-called IMEX methods, and in this paper we will revisit the class of IMEX RK methods analyzed before by Ascher et al. [1,2], Kennedy and Carpenter [23,24] (in a somewhat more general context of additive RK schemes), Pareschi and Russo [26,27], Boscarino [4,5], Boscarino and Russo [7], Boscarino et al. [6], and Cardone et al. [11], and systematically analyze such methods up to the order $p = 4$. We refer to the monograph [9] for the general theory of RK methods.

IMEX two-step Runge–Kutta (TSRK) methods [21] were analyzed by Zharovsky et al. [34], and IMEX general linear methods (GLMs) [20] were analyzed by Zhang and Sandu [32,33], and Cardone et al. [10,12].

The organization of this paper is as follows. In Section 2 we introduce the class of IMEX RK methods and review the order conditions for these schemes. In Section 3 we present the stability analysis of these methods. Design criteria for IMEX RK methods are discussed in Section 4, and the construction of IMEX RK schemes with $p = 2$, $s = 2$, $p = 2$, $s = 3$, $p = 3$, $s = 3$, $p = 3$, $s = 6$, and $p = 4$, $s = 8$, is described in Sections 5.1–5.5. The results of numerical experiments are presented in Section 6 and in Section 7 some concluding remarks are given.

2. IMEX RK methods

Let N be a positive integer and define the stepsize $h = (T - t_0)/N$, and the uniform grid $t_i = t_0 + ih$, $i = 0, 1, \ldots, N$. The IMEX RK methods with s stages are defined by

$$\begin{cases} Y_i = y_n + h\sum_{j=1}^{i-1} \overline{a}_{ij} F_j + h\sum_{j=1}^{i} a_{ij} G_j, \qquad i = 1, 2, \ldots, s, \\ y_{n+1} = y_n + h\sum_{j=1}^{s} \overline{b}_j F_j + h\sum_{j=1}^{s} b_j G_j, \end{cases} \tag{2.1}$$

$n = 0, 1, \ldots, N$. Here,

$$F_j = f(Y_j), \quad G_j = g(Y_j), \quad j = 1, 2, \ldots, s.$$

The explicit part of the IMEX method (2.1) can be represented by the abscissa vector $\overline{\mathbf{c}}$, the strictly lower triangular coefficient matrix $\overline{\mathbf{A}}$, and the vector of weights $\overline{\mathbf{b}}$,

$$\begin{array}{c|c} \overline{\mathbf{c}} & \overline{\mathbf{A}} \\ \hline & \overline{\mathbf{b}}^T \end{array} = \begin{array}{c|cccccc} \overline{c}_1 = 0 & & & & & & \\ \overline{c}_2 & \overline{a}_{21} & & & & & \\ \overline{c}_3 & \overline{a}_{31} & \overline{a}_{32} & & & & \\ \vdots & \vdots & \vdots & \ddots & & & \\ \overline{c}_s & \overline{a}_{s,1} & \overline{a}_{s,2} & \cdots & \overline{a}_{s,s-1} & & \\ \hline & \overline{b}_1 & \overline{b}_2 & \cdots & \overline{b}_{s-1} & \overline{b}_s \end{array}, \tag{2.2}$$

and the implicit part of (2.1) can be represented by the abscissa vector $\mathbf{c}$, the lower triangular coefficient matrix $\mathbf{A}$ with a constant diagonal, and the vector of weights $\mathbf{b}$,

$$\begin{array}{c|c} \mathbf{c} & \mathbf{A} \\ \hline & \mathbf{b}^T \end{array} = \begin{array}{c|ccccc} c_1 & \lambda & & & & \\ c_2 & a_{21} & \lambda & & & \\ c_3 & a_{31} & a_{32} & \lambda & & \\ \vdots & \vdots & \vdots & \ddots & \ddots & \\ c_s & a_{s,1} & a_{s,2} & \cdots & a_{s,s-1} & \lambda \\ \hline & b_1 & b_2 & \cdots & b_{s-1} & b_s \end{array}. \tag{2.3}$$

Putting

$$Y = \begin{bmatrix} Y_1 \\ \vdots \\ Y_s \end{bmatrix}, \quad F = \begin{bmatrix} F_1 \\ \vdots \\ F_s \end{bmatrix}, \quad G = \begin{bmatrix} G_1 \\ \vdots \\ G_s \end{bmatrix},$$

the method (2.1) can be written in a more compact vector form

Table 2.1
Order conditions for IMEX RK methods for $p \leq 3$.

Order	Order conditions for IMEX RK methods	
$p=1$	$\overline{\mathbf{b}}^T\mathbf{e}=1$	$\mathbf{b}^T\mathbf{e}=1$
$p=2$	$\overline{\mathbf{b}}^T\overline{\mathbf{c}}=\frac{1}{2}$	$\mathbf{b}^T\overline{\mathbf{c}}=\frac{1}{2}$
$p=2$	$\overline{\mathbf{b}}^T\mathbf{c}=\frac{1}{2}$	$\mathbf{b}^T\mathbf{c}=\frac{1}{2}$
$p=3$	$\overline{\mathbf{b}}^T\overline{\mathbf{c}}^2=\frac{1}{3}$	$\mathbf{b}^T\overline{\mathbf{c}}^2=\frac{1}{3}$
$p=3$	$\overline{\mathbf{b}}^T(\overline{\mathbf{c}}\cdot\mathbf{c})=\frac{1}{3}$	$\mathbf{b}^T(\overline{\mathbf{c}}\cdot\mathbf{c})=\frac{1}{3}$
$p=3$	$\overline{\mathbf{b}}^T\mathbf{c}^2=\frac{1}{3}$	$\mathbf{b}^T\mathbf{c}^2=\frac{1}{3}$
$p=3$	$\overline{\mathbf{b}}^T\overline{\mathbf{A}}\overline{\mathbf{c}}=\frac{1}{6}$	$\mathbf{b}^T\overline{\mathbf{A}}\overline{\mathbf{c}}=\frac{1}{6}$
$p=3$	$\overline{\mathbf{b}}^T\overline{\mathbf{A}}\mathbf{c}=\frac{1}{6}$	$\mathbf{b}^T\overline{\mathbf{A}}\mathbf{c}=\frac{1}{6}$
$p=3$	$\overline{\mathbf{b}}^T\mathbf{A}\overline{\mathbf{c}}=\frac{1}{6}$	$\mathbf{b}^T\mathbf{A}\overline{\mathbf{c}}=\frac{1}{6}$
$p=3$	$\overline{\mathbf{b}}^T\mathbf{A}\mathbf{c}=\frac{1}{6}$	$\mathbf{b}^T\mathbf{A}\mathbf{c}=\frac{1}{6}$

Table 2.2
Order conditions for IMEX RK methods for $p=4$.

Order	Order conditions for IMEX RK methods	
$p=4$	$\overline{\mathbf{b}}^T\overline{\mathbf{c}}^3=\frac{1}{4}$	$\mathbf{b}^T\overline{\mathbf{c}}^3=\frac{1}{4}$
$p=4$	$\overline{\mathbf{b}}^T(\overline{\mathbf{c}}^2\cdot\mathbf{c})=\frac{1}{4}$	$\mathbf{b}^T(\overline{\mathbf{c}}^2\cdot\mathbf{c})=\frac{1}{4}$
$p=4$	$\overline{\mathbf{b}}^T(\overline{\mathbf{c}}\cdot\mathbf{c}^2)=\frac{1}{4}$	$\mathbf{b}^T(\overline{\mathbf{c}}\cdot\mathbf{c}^2)=\frac{1}{4}$
$p=4$	$\overline{\mathbf{b}}^T\mathbf{c}^3=\frac{1}{4}$	$\mathbf{b}^T\mathbf{c}^3=\frac{1}{4}$
$p=4$	$(\overline{\mathbf{b}}\cdot\overline{\mathbf{c}})^T\overline{\mathbf{A}}\overline{\mathbf{c}}=\frac{1}{8}$	$(\mathbf{b}\cdot\overline{\mathbf{c}})^T\overline{\mathbf{A}}\overline{\mathbf{c}}=\frac{1}{8}$
$p=4$	$(\overline{\mathbf{b}}\cdot\overline{\mathbf{c}})^T\overline{\mathbf{A}}\mathbf{c}=\frac{1}{8}$	$(\mathbf{b}\cdot\overline{\mathbf{c}})^T\overline{\mathbf{A}}\mathbf{c}=\frac{1}{8}$
$p=4$	$(\overline{\mathbf{b}}\cdot\overline{\mathbf{c}})^T\mathbf{A}\overline{\mathbf{c}}=\frac{1}{8}$	$(\mathbf{b}\cdot\overline{\mathbf{c}})^T\mathbf{A}\overline{\mathbf{c}}=\frac{1}{8}$
$p=4$	$(\overline{\mathbf{b}}\cdot\overline{\mathbf{c}})^T\mathbf{A}\mathbf{c}=\frac{1}{8}$	$(\mathbf{b}\cdot\overline{\mathbf{c}})^T\mathbf{A}\mathbf{c}=\frac{1}{8}$
$p=4$	$(\overline{\mathbf{b}}\cdot\mathbf{c})^T\overline{\mathbf{A}}\overline{\mathbf{c}}=\frac{1}{8}$	$(\mathbf{b}\cdot\mathbf{c})^T\overline{\mathbf{A}}\overline{\mathbf{c}}=\frac{1}{8}$
$p=4$	$(\overline{\mathbf{b}}\cdot\mathbf{c})^T\overline{\mathbf{A}}\mathbf{c}=\frac{1}{8}$	$(\mathbf{b}\cdot\mathbf{c})^T\overline{\mathbf{A}}\mathbf{c}=\frac{1}{8}$
$p=4$	$(\overline{\mathbf{b}}\cdot\mathbf{c})^T\mathbf{A}\overline{\mathbf{c}}=\frac{1}{8}$	$(\mathbf{b}\cdot\mathbf{c})^T\mathbf{A}\overline{\mathbf{c}}=\frac{1}{8}$
$p=4$	$(\overline{\mathbf{b}}\cdot\mathbf{c})^T\mathbf{A}\mathbf{c}=\frac{1}{8}$	$(\mathbf{b}\cdot\mathbf{c})^T\mathbf{A}\mathbf{c}=\frac{1}{8}$
$p=4$	$\overline{\mathbf{b}}^T\overline{\mathbf{A}}\overline{\mathbf{c}}^2=\frac{1}{12}$	$\mathbf{b}^T\overline{\mathbf{A}}\overline{\mathbf{c}}^2=\frac{1}{12}$
$p=4$	$\overline{\mathbf{b}}^T\overline{\mathbf{A}}(\overline{\mathbf{c}}\cdot\mathbf{c})=\frac{1}{12}$	$\mathbf{b}^T\overline{\mathbf{A}}(\overline{\mathbf{c}}\cdot\mathbf{c})=\frac{1}{12}$
$p=4$	$\overline{\mathbf{b}}^T\overline{\mathbf{A}}\mathbf{c}^2=\frac{1}{12}$	$\mathbf{b}^T\overline{\mathbf{A}}\mathbf{c}^2=\frac{1}{12}$
$p=4$	$\overline{\mathbf{b}}^T\mathbf{A}\overline{\mathbf{c}}^2=\frac{1}{12}$	$\mathbf{b}^T\mathbf{A}\overline{\mathbf{c}}^2=\frac{1}{12}$
$p=4$	$\overline{\mathbf{b}}^T\mathbf{A}(\overline{\mathbf{c}}\cdot\mathbf{c})=\frac{1}{12}$	$\mathbf{b}^T\mathbf{A}(\overline{\mathbf{c}}\cdot\mathbf{c})=\frac{1}{12}$
$p=4$	$\overline{\mathbf{b}}^T\mathbf{A}\mathbf{c}^2=\frac{1}{12}$	$\mathbf{b}^T\mathbf{A}\mathbf{c}^2=\frac{1}{12}$
$p=4$	$\overline{\mathbf{b}}^T\overline{\mathbf{A}}^2\overline{\mathbf{c}}=\frac{1}{24}$	$\mathbf{b}^T\overline{\mathbf{A}}^2\overline{\mathbf{c}}=\frac{1}{24}$
$p=4$	$\overline{\mathbf{b}}^T\overline{\mathbf{A}}\overline{\mathbf{A}}\overline{\mathbf{c}}=\frac{1}{24}$	$\mathbf{b}^T\overline{\mathbf{A}}\overline{\mathbf{A}}\overline{\mathbf{c}}=\frac{1}{24}$
$p=4$	$\overline{\mathbf{b}}^T\overline{\mathbf{A}}^2\mathbf{c}=\frac{1}{24}$	$\mathbf{b}^T\overline{\mathbf{A}}^2\mathbf{c}=\frac{1}{24}$
$p=4$	$\overline{\mathbf{b}}^T\overline{\mathbf{A}}\overline{\mathbf{A}}\mathbf{c}=\frac{1}{24}$	$\mathbf{b}^T\overline{\mathbf{A}}\overline{\mathbf{A}}\mathbf{c}=\frac{1}{24}$
$p=4$	$\overline{\mathbf{b}}^T\mathbf{A}\overline{\mathbf{A}}\overline{\mathbf{c}}=\frac{1}{24}$	$\mathbf{b}^T\mathbf{A}\overline{\mathbf{A}}\overline{\mathbf{c}}=\frac{1}{24}$
$p=4$	$\overline{\mathbf{b}}^T\mathbf{A}^2\overline{\mathbf{c}}=\frac{1}{24}$	$\mathbf{b}^T\mathbf{A}^2\overline{\mathbf{c}}=\frac{1}{24}$
$p=4$	$\overline{\mathbf{b}}^T\mathbf{A}\overline{\mathbf{A}}\mathbf{c}=\frac{1}{24}$	$\mathbf{b}^T\mathbf{A}\overline{\mathbf{A}}\mathbf{c}=\frac{1}{24}$
$p=4$	$\overline{\mathbf{b}}^T\mathbf{A}^2\mathbf{c}=\frac{1}{24}$	$\mathbf{b}^T\mathbf{A}^2\mathbf{c}=\frac{1}{24}$

$$\begin{cases} Y=(\mathbf{e}\otimes\mathbf{I})y_n+h(\overline{\mathbf{A}}\otimes\mathbf{I})F+h(\mathbf{A}\otimes\mathbf{I})G, \\ y_{n+1}=y_n+h(\overline{\mathbf{b}}^T\otimes\mathbf{I})F+h(\mathbf{b}^T\otimes\mathbf{I})G, \end{cases} \tag{2.4}$$

$n=0,1,\ldots,N-1$, where $\mathbf{e}=[1,\ldots,1]^T\in\mathbb{R}^s$, and $\mathbf{I}$ is the identity matrix of dimension s.

The order conditions for IMEX RK methods (2.4) were derived in [1,23,24,27]. For easy reference these order conditions up to the order $p=3$ are listed in Table 2.1 and order conditions for $p=4$ are listed in Table 2.2.

3. Stability analysis of IMEX RK methods

To analyze stability properties of IMEX RK methods (2.4) we consider the test equation

$$y'(t) = \lambda_0 y(t) + \lambda_1 y(t), \quad t \geq 0, \tag{3.1}$$

$\lambda_0, \lambda_1 \in \mathbb{C}$, where $\lambda_0 y(t)$ corresponds to the non stiff part and $\lambda_1 y(t)$ to the stiff part of the problem (1.1). Applying (2.4) to (3.1) we obtain

$$\begin{cases} Y = y_n \mathbf{e} + z_0 \overline{\mathbf{A}} Y + z_1 \mathbf{A} Y, \\ y_{n+1} = y_n + z_0 \overline{\mathbf{b}}^T Y + z_1 \mathbf{b}^T Y, \end{cases} \tag{3.2}$$

$n = 0, 1, \ldots$, where we have used the notation $z_0 = h\lambda_0$, $z_1 = h\lambda_1$.

Assuming that $\det(\mathbf{I} - z_0 \overline{\mathbf{A}} - z_1 \mathbf{A}) \neq 0$ it follows from the first equation of (3.2) that

$$Y = (\mathbf{I} - z_0 \overline{\mathbf{A}} - z_1 \mathbf{A})^{-1} \mathbf{e} y_n,$$

and substituting this relation into the second equation of (3.2) we obtain

$$y_{n+1} = R(z_0, z_1) y_n, \tag{3.3}$$

$n = 0, 1, \ldots$, where the stability function $R(z_0, z_1)$ is defined by

$$R(z_0, z_1) = 1 + (z_0 \overline{\mathbf{b}}^T + z_1 \mathbf{b}^T)(\mathbf{I} - z_0 \overline{\mathbf{A}} - z_1 \mathbf{A})^{-1} \mathbf{e}. \tag{3.4}$$

For IMEX RK methods (2.1) with coefficients defined by (2.2) and (2.3) this function takes the form

$$R(z_0, z_1) = \frac{P(z_0, z_1)}{(1 - \lambda z_1)^s},$$

where $p(z_0, z_1)$ is a polynomial of degree s with respect to z_0 and z_1. For $z_0 = 0$ we have

$$R(0, z_1) = 1 + z_1 \mathbf{b}^T (\mathbf{I} - z_1 \mathbf{A})^{-1} \mathbf{e} = \frac{P(0, z_1)}{(1 - \lambda z_1)^s},$$

which is the stability function of diagonally implicit RK method (2.3). For $z_1 = 0$ we have

$$R(z_0, 0) = 1 + z_0 \overline{\mathbf{b}}^T (\mathbf{I} - z_0 \overline{\mathbf{A}})^{-1} \mathbf{e} = P(z_0, 0),$$

which is the stability polynomial of explicit RK method (2.2).

As observed in [16] (see also [10–12]) in the context of IMEX θ-methods good stability properties of explicit method (2.2) and implicit method (2.3) are not sufficient to guarantee desirable stability properties of the overall IMEX scheme (2.1), and it is necessary to investigate stability properties of these methods when both explicit and implicit RK formulas operate in tandem as IMEX scheme. We are mainly interested in constructing methods which are $A(\alpha)$- or A-stable with respect to the implicit part $z_1 \in \mathbb{C}$ and have large regions of stability with respect to the explicit part $z_0 \in \mathbb{C}$. To investigate methods with these properties we define the appropriate stability regions which are subsets of $\mathbb{C}^2$ or $\mathbb{C}$. The region of absolute stability of the scheme (2.1) is defined as

$$\mathcal{A} = \left\{ (z_0, z_1) \in \mathbb{C}^2 : \ \left| R(z_0, z_1) \right| \leq 1 \right\}.$$

For $\alpha \in (0, \pi/2]$ we also define the following subsets of $\mathbb{C}$

$$\mathcal{A}_\alpha = \left\{ z \in \mathbb{C} : \ \mathrm{Re}(z) < 0 \text{ and } \left| \mathrm{Im}(z) \right| \leq \tan(\alpha) \left| \mathrm{Re}(z) \right| \right\},$$

and

$$\mathcal{S}_\alpha = \left\{ z_0 \in \mathbb{C} : \ \left| R(z_0, z_1) \right| \leq 1 \text{ for } z_1 \in \mathcal{A}_\alpha \right\}.$$

We can interpret $\mathcal{S}_\alpha$ as the region of absolute stability of the explicit part of (2.1) assuming that the implicit part of (2.1) is $A(\alpha)$-stable. In particular, $\mathcal{S}_{\pi/2}$ is the stability region of explicit part of (2.1) assuming that the implicit part of (2.1) is A-stable.

For fixed $y \in \mathbb{R}$ we also define the set

$$\mathcal{S}_{\alpha, y} = \left\{ z_0 \in \mathbb{C} : \ \left| R(z_0, z_1) \right| \leq 1 \text{ for } z_1 = -|y| / \tan(\alpha) + iy \right\}.$$

The set $\mathcal{S}_{\alpha, 0}$ corresponding to $y = 0$ is independent of α, and it is equal to the region of absolute stability of the explicit RK method (2.2). This set will be denoted by $\mathcal{S}_E$. We have

$$\mathcal{S}_\alpha \subset \mathcal{S}_E,$$

and similarly as in [10–12], we will search for IMEX RK schemes (2.1) for which $\mathcal{S}_\alpha$ contains a large part of $\mathcal{S}_E$ for some $\alpha \in (0, \pi/2]$, preferably for $\alpha = \pi/2$. The design criteria of IMEX RK methods are discussed in Section 4.

Similarly as in [10–12] the boundary $\partial\mathcal{S}_{\alpha,y}$ of $\mathcal{S}_{\alpha,y}$ can be computed by the boundary locus method which computes the locus of the curve

$$\partial\mathcal{S}_{\alpha,y} = \left\{ z_0 \in \mathbb{C} : \ R\big(z_0, -|y|/\tan(\alpha) + iy\big) = e^{i\theta}, \ \theta \in [0, 2k\pi] \right\},$$

where k is a positive integer. In [10] we described also an algorithm to compute the boundary $\partial\mathcal{S}_\alpha$ of the stability region $\mathcal{S}_\alpha$ for $\alpha \in (0, \pi/2]$. This algorithm is based on the relation

$$\mathcal{S}_\alpha = \bigcap_{y \in \mathbb{R}} \mathcal{S}_{\alpha,y}, \tag{3.5}$$

which follows from the maximum principle. In this algorithm for fixed direction $m = -\tan(\alpha)$, and for fixed $z_1 = -|y|/\tan(\alpha) + iy$ we compute, by the bisection method, the intersection of the boundary $\partial\mathcal{S}_{\alpha,y}$ with the ray $y_0 = -\tan(\alpha)x_0$. Then we look for a point $\overline{z}_0 \in \mathbb{C}$ with minimum value of $\overline{y}_0 = -\mathrm{Im}(\overline{z}_0)$. Such a point belongs to the boundary $\partial\mathcal{S}_\alpha$ of the stability region $\mathcal{S}_\alpha$. We refer to [10] for a detailed description of this algorithm. A somewhat different approach to compute $\partial\mathcal{S}_\alpha$ is presented in [26].

4. Design criteria for IMEX RK methods

In this section we describe the design criteria which will be used to construct IMEX RK schemes (2.1) with some desirable stability properties.

The first design criterion is based on maximizing the area of the region of absolute stability $\mathcal{S}_E$ of explicit RK method (2.2). This area can be computed by numerical integration in polar coordinates as described in [3]. Such methods are obtained by the solution of the minimization problem

$$-\mathrm{area}(\mathcal{S}_E) \longrightarrow \min, \tag{4.1}$$

with equality constrains

$$\Phi_p(\overline{\mathbf{c}}, \overline{\mathbf{A}}, \overline{\mathbf{b}}, \mathbf{c}, \mathbf{A}, \mathbf{b}) = 0, \tag{4.2}$$

where the function Φ_p represents order conditions up to the order p. These order conditions are listed in Table 2.1 for $p \le 3$ and in Table 2.2 for $p = 4$.

The second criterion is based on maximizing the area of $\mathcal{S}_\alpha$ for fixed $\alpha \in (0, \pi/2]$. Such methods are obtained by the solution of the minimization problem

$$-\mathrm{area}(\mathcal{S}_\alpha) \longrightarrow \min, \tag{4.3}$$

$\alpha \in (0, \pi/2]$, with the same as before equality constrains (4.2).

The third design criterion is based on maximizing the strong stability preserving (SSP) coefficient of the explicit RK method (2.2). This leads to the so-called SSP methods, compare [13,14]. To describe this criterion assume that the discretization of the problem (1.1) with $g(y) \equiv 0$ by the forward Euler method

$$y_{n+1} = y_n + hf(y_n),$$

$n = 0, 1, \ldots, N-1$, satisfies the monotonicity condition

$$\|y_{n+1}\| \le \|y_n\| \tag{4.4}$$

in some norm or seminorm $\|\cdot\|$, for a suitably restricted time step h determined by the CFL condition

$$h \le h_{FE}. \tag{4.5}$$

Then we will look for IMEX RK schemes of order p such that the explicit part (2.2) of the scheme preserve the monotonicity property (4.4), under the perhaps modified restriction on the step size h

$$h \le \mathcal{C} \cdot h_{FE} \tag{4.6}$$

measured by the SSP coefficient $\mathcal{C} \ge 0$ of the explicit RK method (2.2). Consider the RK method (2.2) and define the matrices

$$\overline{\mathbf{T}} = \left[\begin{array}{c|c} \overline{\mathbf{A}} & \mathbf{0} \\ \hline \overline{\mathbf{b}}^T & 0 \end{array}\right] \in \mathbb{R}^{(s+1)\times(s+1)}, \quad \overline{\mathbf{S}} = \left[\begin{array}{c} \mathbf{e} \\ \hline 1 \end{array}\right] \in \mathbb{R}^{s+1}.$$

These are the coefficient matrices of the representation of RK method (2.2) as general linear method (GLM) which was considered by Spijker [31]. Denote by $\mathbf{I}$ the identity matrix of dimension $s+1$, and let $[\overline{\mathbf{S}}|\gamma\overline{\mathbf{T}}]$, $\gamma \in \mathbb{R}$, stand for the $(s+1) \times$

$(s+2)$ matrix whose first column is equal to $\overline{\mathbf{S}}$ and the last $s+1$ columns are equal to $\gamma\overline{\mathbf{T}}$. Next, following Spijker [31] we consider the conditions

$$\det(\mathbf{I}+\gamma\overline{\mathbf{T}})\neq 0 \quad \text{and} \quad (\mathbf{I}+\gamma\overline{\mathbf{T}})^{-1}\left[\,\overline{\mathbf{S}}\;\middle|\;\gamma\overline{\mathbf{T}}\,\right]\geq 0, \tag{4.7}$$

where the above inequality should be interpreted componentwise. Then it follows from the result by Spijker [31] that the SSP coefficient of the method (2.2) (or, in general, of the GLM defined by $\overline{\mathbf{T}}$ and $\overline{\mathbf{S}}$) is given by

$$\mathcal{C}=\mathcal{C}(\overline{\mathbf{T}},\overline{\mathbf{S}})=\sup\left\{\gamma\in\mathbb{R}:\ \gamma \text{ satisfies (4.7)}\right\}. \tag{4.8}$$

The conditions (4.7) can be reformulated in terms of $\overline{\mathbf{A}}$ and $\overline{\mathbf{b}}$. Since $\overline{\mathbf{A}}$ is strictly lower triangular we have $\det(\mathbf{I}+\gamma\overline{\mathbf{A}})\neq 0$ which implies that $\det(\mathbf{I}+\gamma\overline{\mathbf{T}})\neq 0$, and it can be verified that the conditions (4.7) can be reformulated as

$$\begin{aligned}&\left(\mathbf{I}+\gamma\overline{\mathbf{A}}\right)^{-1}\mathbf{e}\geq 0,\quad \mathbf{I}-\left(\mathbf{I}+\gamma\overline{\mathbf{A}}\right)^{-1}\geq 0,\\ &1-\gamma\overline{\mathbf{b}}^{T}\left(\mathbf{I}+\gamma\overline{\mathbf{A}}\right)^{-1}\mathbf{e}\geq 0,\quad \gamma\overline{\mathbf{b}}^{T}\left(\mathbf{I}+\gamma\overline{\mathbf{A}}\right)^{-1}\geq 0.\end{aligned} \tag{4.9}$$

Then it follows that the characterization of the SSP coefficient (4.8) for the representation of RK method (2.2) as GLM with coefficients $\overline{\mathbf{T}}$ and $\overline{\mathbf{S}}$ can be reformulated in terms of $\overline{\mathbf{A}}$ and $\overline{\mathbf{b}}$ as

$$\mathcal{C}=\mathcal{C}(\overline{\mathbf{A}},\overline{\mathbf{b}})=\sup\left\{\gamma\in\mathbb{R}:\ \gamma \text{ satisfies (4.9)}\right\}. \tag{4.10}$$

Similarly as in [17–19,25], this coefficient can be computed by the solution to the constrained minimization problem

$$F(\gamma,\overline{\mathbf{c}},\overline{\mathbf{A}},\overline{\mathbf{b}},\mathbf{c},\mathbf{A},\mathbf{b})=-\gamma\longrightarrow\min, \tag{4.11}$$

with inequality constrains (4.9) and equality constrains (4.2) in the form of order conditions up to the order p.

5. Construction of IMEX RK methods

In this section we describe the construction of highly stable IMEX RK schemes up to the order $p=4$ using the design criteria which were discussed in Section 4.

5.1. IMEX RK schemes with $p=2$ and $s=2$

Solving the order conditions up to $p=2$ we obtain a two-parameter family of IMEX RK schemes with coefficients

$$\begin{array}{c|c|cc}\overline{\mathbf{c}}&\overline{\mathbf{A}}&0&\\ &&\frac{a_{21}}{1-2\lambda}&\frac{a_{21}}{1-2\lambda}\\ \hline &\overline{\mathbf{b}}^{T}&\frac{2\lambda+2a_{21}-1}{2a_{21}}&\frac{1-2\lambda}{2a_{21}}\end{array}=\begin{array}{c|c|cc}\mathbf{c}&\mathbf{A}&\lambda&\\ &&a_{21}+\lambda&\lambda\\ \hline &\mathbf{b}^{T}&\frac{2\lambda+2a_{21}-1}{2a_{21}}&\frac{1-2\lambda}{2a_{21}}\end{array},\qquad \begin{array}{c|c|cc}\mathbf{c}&\mathbf{A}&\lambda&\\ &&a_{21}&\lambda\\ \hline &\mathbf{b}^{T}&\frac{2\lambda+2a_{21}-1}{2a_{21}}&\frac{1-2\lambda}{2a_{21}}\end{array}.$$

The stability function of this scheme is $R(z_0,z_1)=P(z_0,z_1)/Q(z_0,z_1)$ with

$$P(z_0,z_1)=1+z_0+\frac{z_0^2}{2}+(1-2\lambda)z_1+(1-2\lambda)z_0z_1+\left(\frac{1}{2}-2\lambda+\lambda^2\right)z_1^2,$$

and

$$Q(z_0,z_1)=(1-\lambda z_1)^2.$$

The Nørsett polynomial [15] of the implicit part of the scheme corresponding to $z_0=0$ is independent of a_{21} and is given by

$$E(y):=Q(0,iy)Q(0,-iy)-P(0,iy)P(0,-iy)=\left(\lambda-\frac{1}{4}\right)(1-2\lambda)^2y^4.$$

Hence, it follows that the implicit RK method is A-stable if and only if $\lambda\geq 1/4$. Moreover, this method is L-stable if and only if $\lambda=(2\pm\sqrt{2})/2$, which are the roots of the polynomial $\lambda^2-2\lambda+1/2$.

Choosing $a_{21}=1/(1-2\lambda)$ we obtain a one parameter family of IMEX schemes of order $p=2$ proposed by Pareschi and Russo [27]. The coefficients of these methods are given by

$$\begin{array}{c|c|cc}\overline{\mathbf{c}}&\overline{\mathbf{A}}&0&\\ &&1&1\\ \hline &\overline{\mathbf{b}}^{T}&\frac{1}{2}&\frac{1}{2}\end{array}=\begin{array}{c|c|cc}\mathbf{c}&\mathbf{A}&\lambda&\\ &&1-\lambda&1-2\lambda\quad\lambda\\ \hline &\mathbf{b}^{T}&\frac{1}{2}&\frac{1}{2}\end{array}.$$

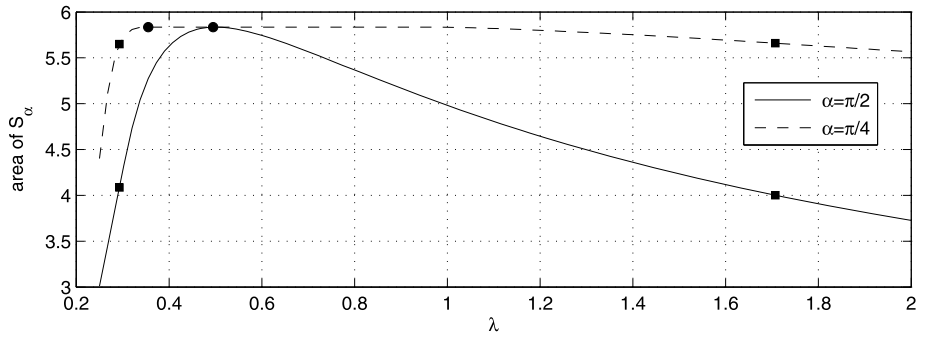

Fig. 5.1. Area of stability region $\mathcal{S}_\alpha$ versus λ for $\alpha = \pi/2$ and $\alpha = \pi/4$.

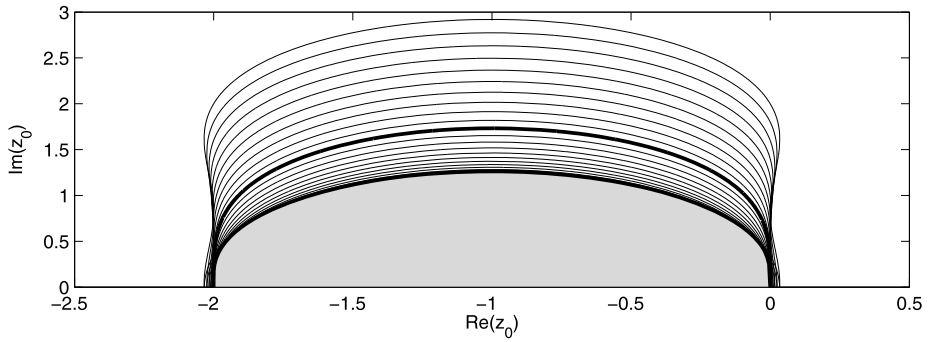

Fig. 5.2. Stability regions $\mathcal{S}_{\pi/2,y}$, $y = -2.0, -1.8, \ldots, 2.0$ (thin lines), $\mathcal{S}_{\pi/2}$ (shaded region) for $\lambda = (2-\sqrt{2})/2$, and $\mathcal{S}_E$ (thick line) of the IMEX scheme with $p = 2$ and $s = 2$.

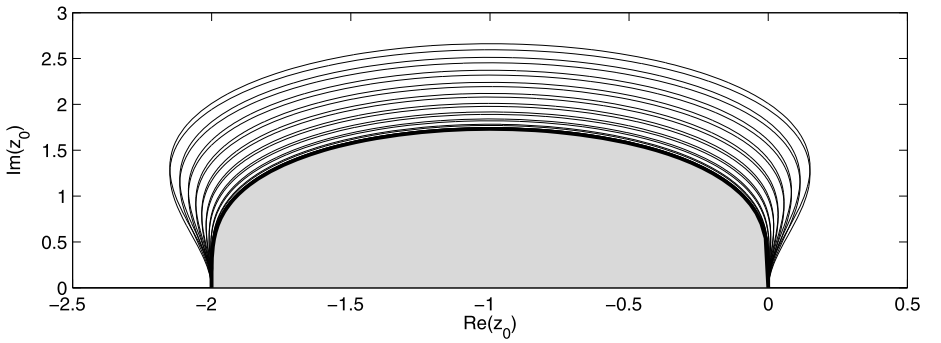

Fig. 5.3. Stability regions $\mathcal{S}_{\pi/2,y}$, $y = -2.0, -1.8, \ldots, 2.0$ (thin lines), $\mathcal{S}_{\pi/2}$ (shaded region) for $\lambda = 0.4918055243674397$, and $\mathcal{S}_E$ (thick line) of the IMEX scheme with $p = 2$ and $s = 2$.

It can be verified that the explicit RK method has SSP property with the effective SSP coefficient $\mathcal{C}_{eff} = \mathcal{C}/s$, i.e., SSP coefficient $\mathcal{C}$ scaled by the number of stages s, equal to $\mathcal{C}_{eff} = 1/2$. This is equal to the optimal value $(s-1)/s = 1/2$ for explicit RK method of order $p = 2$ with $s = 2$ stages, compare [13].

We have plotted on Fig. 5.1 the area of the stability region $\mathcal{S}_\alpha$ versus λ for $\alpha = \pi/2$ and $\alpha = \pi/4$. For $\alpha = \pi/2$ this area attains its maximum values approximately equal to 5.83 for $\lambda = 0.4918055243674397$, and for $\alpha = \pi/4$ this area attains its maximum value again approximately equal to 5.83 for $\lambda = 0.345$. The resulting methods will be denoted by IMEX-RK22$\mathcal{S}_{\pi/2}$ and IMEX-RK22$\mathcal{S}_{\pi/4}$. The points corresponding to these methods are marked by the black circles on Fig. 5.1. We have also marked by the black squares the points corresponding to the L-stable implicit RK methods. These points are $\lambda = (2-\sqrt{2})/2$ for which the area of $\mathcal{S}_\alpha$ is approximately equal to 4.09 for $\alpha = \pi/2$ and approximately equal to 5.65 for $\alpha = \pi/4$, and $\lambda = (2+\sqrt{2})/2$ for which the area of $\mathcal{S}_\alpha$ is approximately equal to 4.00 for $\alpha = \pi/2$, and approximately equal to 5.66 for $\alpha = \pi/4$. The IMEX schemes corresponding to these values of λ are denoted by IMRX-RK22Lm and IMRX-RK22Lp, respectively. We have also plotted on Fig. 5.2 stability region $\mathcal{S}_{\pi/2}$ corresponding to $\lambda = (2-\sqrt{2})/2$ (shaded region) and stability region $\mathcal{S}_E$ of the explicit method (thick line). To illustrate the relation (3.5) we have also plotted by thin lines stability regions $\mathcal{S}_{\pi/2,y}$ for $y = -2.0, -1.8, \ldots, 2.0$. On Fig. 5.3 we have plotted stability region $\mathcal{S}_{\pi/2}$ corresponding to

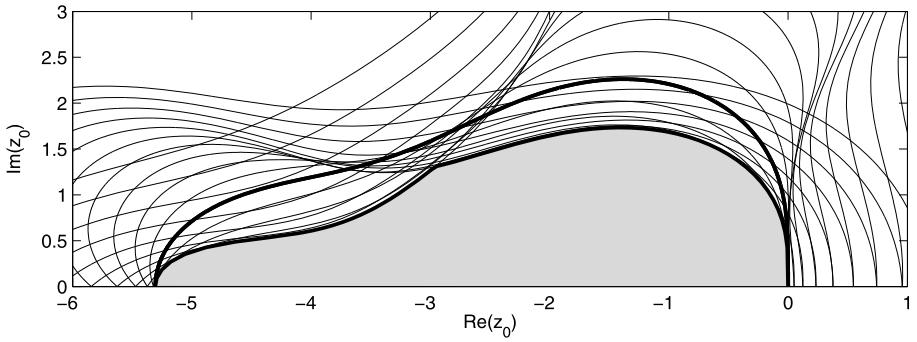

Fig. 5.4. Stability regions $\mathcal{S}_{\pi/2,y}$, $y=-2.0,-1.8,\ldots,2.0$ (thin lines), $\mathcal{S}_{\pi/2}$ (shaded region), and $\mathcal{S}_E$ (thick line) for the IMEX scheme with $p=2$ and $s=3$ with maximal area of $\mathcal{S}_E$.

$\lambda=0.4918055243674397$ (shaded region) and stability region $\mathcal{S}_E$ of the explicit method (thick line). As before we have also plotted by thin lines stability regions $\mathcal{S}_{\pi/2,y}$ for $y=-2.0,-1.8,\ldots,2.0$. In this case the regions $\mathcal{S}_{\pi/2}$ and $\mathcal{S}_E$ are almost identical and cannot be distinguished on Fig. 5.3.

5.2. IMEX RK schemes with $p=2$ and $s=3$

Solving the order conditions up to $p=2$ we obtain a six-parameter family of IMEX RK schemes with coefficients

$$\begin{array}{c|c}\overline{\mathbf{c}} & \overline{\mathbf{A}}\\ \hline & \overline{\mathbf{b}}^T\end{array}=\begin{array}{c|ccc}0 & & & \\ \overline{a}_{21} & \overline{a}_{21} & & \\ \overline{a}_{31}+\overline{a}_{32} & \overline{a}_{31} & \overline{a}_{32} & \\ \hline & \overline{b}_1 & \overline{b}_2 & \overline{b}_3\end{array},\qquad \begin{array}{c|c}\mathbf{c} & \mathbf{A}\\ \hline & \mathbf{b}^T\end{array}=\begin{array}{c|ccc}\lambda & \lambda & & \\ a_{21}+\lambda & a_{21} & \lambda & \\ a_{31}+a_{32}+\lambda & a_{31} & a_{32} & \lambda \\ \hline & b_1 & b_2 & b_3\end{array},$$

where $\overline{b}_1$, $\overline{b}_2$, $\overline{b}_3$, b_1, b_2, and b_3 depend on the free parameters $\overline{a}_{21}$, $\overline{a}_{31}$, $\overline{a}_{32}$, a_{21}, a_{31}, and a_{32}.

We will search first for IMEX schemes with maximal area of the region of absolute stability $\mathcal{S}_E$ of the explicit method $(\overline{\mathbf{c}},\overline{\mathbf{A}},\overline{\mathbf{b}})$. Solving the minimization problem (4.1) we obtain the IMEX scheme with coefficients

$$\begin{aligned}
\overline{\mathbf{c}}&=\begin{bmatrix}0 & 1.001189204627373 & 0.838063598174237\end{bmatrix}^T,\\
\overline{\mathbf{A}}&=\begin{bmatrix}0 & 0 & 0\\ 1.001189204627373 & 0 & 0\\ 0.253545544784129 & 0.584518053390108 & \end{bmatrix},\\
\overline{\mathbf{b}}&=\begin{bmatrix}0.480520005477614 & 0.396275778012860 & 0.123204216509527\end{bmatrix}^T,\\
\mathbf{c}&=\begin{bmatrix}0.743134194610956 & -0.898043878577327 & 4.048418175438741\end{bmatrix}^T,\\
\mathbf{A}&=\begin{bmatrix}0.743134194610956 & 0 & 0\\ -1.641178073188283 & 0.743134194610956 & 0\\ 1.132080119545815 & 2.173203861281970 & 0.743134194610956\end{bmatrix},\\
\mathbf{b}&=\begin{bmatrix}0.480520005477614 & 0.396275778012860 & 0.123204216509527\end{bmatrix}^T.
\end{aligned}$$

This methods will be denoted by IMEX-RK23$\mathcal{S}_E$.

We have plotted on Fig. 5.4 stability region $\mathcal{S}_{\pi/2}$ (shaded region) and stability region $\mathcal{S}_E$ of the explicit method (thick line). We have also plotted by thin lines stability regions $\mathcal{S}_{\pi/2,y}$ for $y=-2.0,-1.8,\ldots,2.0$. The area of $\mathcal{S}_E$ is approximately equal to 16.62 and the area of $\mathcal{S}_{\pi/2}$ is approximately equal to 11.73. It can be verified using (4.9) and (4.10) that the explicit RK method $(\overline{\mathbf{c}},\overline{\mathbf{A}},\overline{\mathbf{b}})$ has SSP property with the effective SSP coefficient $\mathcal{C}_{eff}=0.144$. This is quite far from the optimal value which, for explicit RK method of order $p=2$ with $s=3$ stages, is equal to $(s-1)/s=2/3$, compare [13]. However, we will find IMEX schemes for which the explicit RK method has optimal SSP coefficient using the third design criterion from Section 4. It can be also verified that the implicit method $(\mathbf{c},\mathbf{A},\mathbf{b})$ is A-stable but not L-stable.

We will search next for IMEX schemes with maximal area of the region $\mathcal{S}_\alpha$ for $\alpha=\pi/2$. Solving the minimization problem (4.3) we obtain the IMEX scheme with coefficients

$$\begin{aligned}
\overline{\mathbf{c}}&=\begin{bmatrix}0 & 0.577185900656255 & 1.047384863251074\end{bmatrix}^T,\\
\overline{\mathbf{A}}&=\begin{bmatrix}0 & 0 & 0\\ 0.577185900656255 & 0 & \\ 0.659759720087210 & 0.387625143163863 & 0\end{bmatrix},
\end{aligned}$$

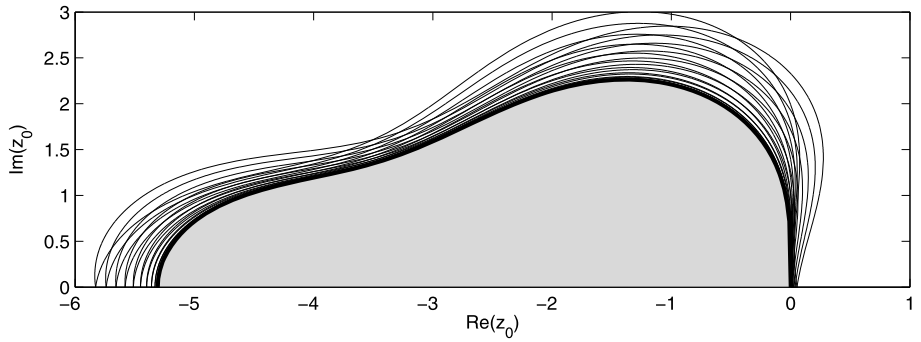

Fig. 5.5. Stability regions $\mathcal{S}_{\pi/2,y}$, $y=-2.0,-1.8,\ldots,2.0$ (thin lines), $\mathcal{S}_{\pi/2}$ (shaded region), and $\mathcal{S}_E$ (thick line) for the IMEX scheme with $p=2$ and $s=3$ with maximal area of $\mathcal{S}_{\pi/2}$.

$$\overline{\mathbf{b}} = \begin{bmatrix} 0.396284461794023 & 0.281418137752127 & 0.322297400453850 \end{bmatrix}^T,$$
$$\mathbf{c} = \begin{bmatrix} 0.331054829332169 & 1.041645102768150 & 0.234784053509575 \end{bmatrix}^T,$$
$$\mathbf{A} = \begin{bmatrix} 0.331054829332169 & 0 & \\ 0.710590273435981 & 0.331054829332169 & 0 \\ -0.126881367560843 & 0.030610591738250 & 0.331054829332169 \end{bmatrix},$$
$$\mathbf{b} = \begin{bmatrix} 0.396284461794023 & 0.281418137752127 & 0.322297400453850 \end{bmatrix}^T.$$

This methods will be denoted by IMEX-RK23$\mathcal{S}_{\pi/2}$.

We have plotted on Fig. 5.5 stability region $\mathcal{S}_{\pi/2}$ (shaded region) and stability region $\mathcal{S}_E$ of the explicit method (thick line). We have also plotted by thin lines stability regions $\mathcal{S}_{\pi/2,y}$ for $y=-2.0,-1.8,\ldots,2.0$. The areas of $\mathcal{S}_E$ and $\mathcal{S}_{\pi/2}$ are approximately equal to 16.62. These areas cannot be distinguished on Fig. 5.5. It can be verified using (4.9) and (4.10) that the explicit RK method $(\overline{\mathbf{c}},\overline{\mathbf{A}},\overline{\mathbf{b}})$ has SSP property with the effective SSP coefficient $\mathcal{C}_{eff}=0.445$. It can be also verified that the implicit method $(\mathbf{c},\mathbf{A},\mathbf{b})$ is A-stable but not L-stable.

Finally, we will search for IMEX schemes for which the explicit RK method $(\overline{\mathbf{c}},\overline{\mathbf{A}},\overline{\mathbf{b}})$ has the maximal SSP coefficient. Solving the minimization problem (4.11) with inequality constrains (4.9) leads to a scheme with coefficients given by

$$\overline{\mathbf{c}} = \begin{bmatrix} 0 \\ \frac{1}{2} \\ 1 \end{bmatrix}, \quad \overline{\mathbf{A}} = \begin{bmatrix} 0 & 0 & 0 \\ \frac{1}{2} & 0 & 0 \\ \frac{1}{2} & \frac{1}{2} & 0 \end{bmatrix}, \quad \overline{\mathbf{b}} = \begin{bmatrix} \frac{1}{3} \\ \frac{1}{3} \\ \frac{1}{3} \end{bmatrix},$$
$$\mathbf{c} = \begin{bmatrix} 0.204976822001215 & 0.686915776921670 & 0.608107401077115 \end{bmatrix}^T,$$
$$\mathbf{A} = \begin{bmatrix} 0.204976822001215 & 0 & 0 \\ 0.481938954920455 & 0.204976822001215 & 0 \\ 0.250998127128454 & 0.152132451947445 & 0.204976822001215 \end{bmatrix},$$
$$\mathbf{b} = \begin{bmatrix} \frac{1}{3} & \frac{1}{3} & \frac{1}{3} \end{bmatrix}^T.$$

This methods will be denoted by IMEX-RK23SSP.

We have plotted on Fig. 5.6 stability region $\mathcal{S}_{\pi/2}$ (shaded region) and stability region $\mathcal{S}_E$ of the explicit method (thick line). We have also plotted by thin lines stability regions $\mathcal{S}_{\pi/2,y}$ for $y=-2.0,-1.8,\ldots,2.0$. The area of $\mathcal{S}_E$ is approximately equal to 15.87 and the area of $\mathcal{S}_{\pi/2}$ is approximately equal to 12.55. We can observe that the area of $\mathcal{S}_E$ and the interval of absolute stability are somewhat smaller than the corresponding areas and intervals of stability of explicit RK methods $(\overline{\mathbf{c}},\overline{\mathbf{A}},\overline{\mathbf{b}})$ obtained by the first two of the design criteria from Section 4. However, in this case the explicit RK method $(\overline{\mathbf{c}},\overline{\mathbf{A}},\overline{\mathbf{b}})$ has SSP property with the optimal effective SSP coefficient $\mathcal{C}_{eff}=(s-1)/s=2/3$. This explicit RK method was also obtained by Pareschi and Russo [27] as explicit part of IMEX scheme with implicit part which is stiffly accurate. It can be also verified that the implicit method $(\mathbf{c},\mathbf{A},\mathbf{b})$ listed above is A-stable but not L-stable.

5.3. IMEX RK schemes with $p=3$ and $s=3$

In this section we consider IMEX schemes with diagonally implicit Runge–Kutta (DIRK) methods with λ_1, λ_2, and λ_3 on the diagonal of the coefficient matrix $\mathbf{A}$. Solving the order conditions up to the order $p=2$ with respect to $\overline{b}_1$, $\overline{b}_2$, $\overline{b}_3$, b_1, b_2, and b_3 leads to methods for which $\overline{\mathbf{b}}=\mathbf{b}$. Solving next order conditions corresponding to $p=3$ with respect to $\overline{a}_{21}$, $\overline{a}_{31}$, $\overline{a}_{32}$, a_{21}, a_{31}, a_{32}, and λ_3 we obtain a two parameter family of methods depending on λ_1, and λ_2. The coefficients of the resulting IMEX scheme are given by

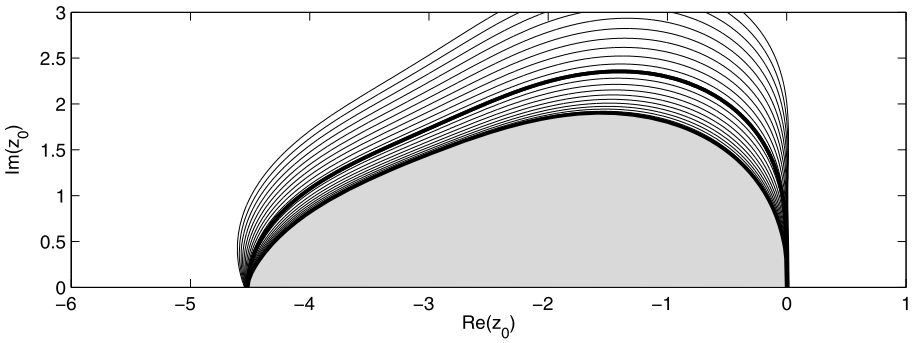

Fig. 5.6. Stability regions $\mathcal{S}_{\pi/2,y}$, $y=-2.0,-1.8,\ldots,2.0$ (thin lines), $\mathcal{S}_{\pi/2}$ (shaded region), and $\mathcal{S}_E$ (thick line) for the IMEX scheme with $p=2$ and $s=3$ with maximal SSP coefficient.

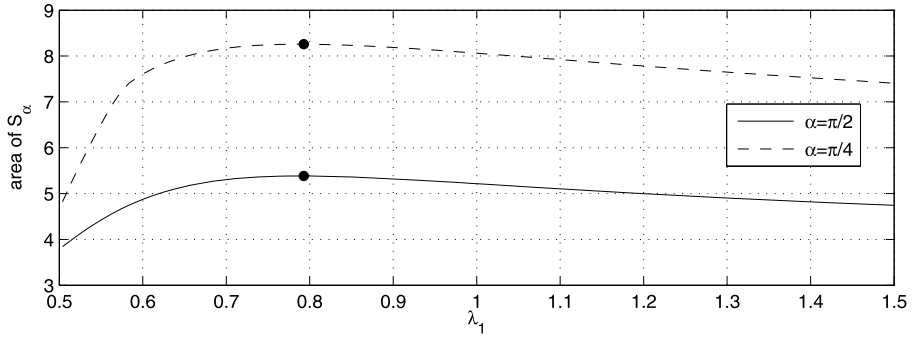

Fig. 5.7. Area of stability region $\mathcal{S}_\alpha$ versus λ_1 for $\alpha=\pi/2$ and $\alpha=\pi/4$.

$$\overline{\mathbf{c}}=\begin{bmatrix}0\\ \frac{1}{3}\\ 1\end{bmatrix},\quad \overline{\mathbf{A}}=\begin{bmatrix}0&0&0\\ \frac{1}{3}&0&0\\ -1&2&0\end{bmatrix},\quad \overline{\mathbf{b}}=\begin{bmatrix}0\\ \frac{3}{4}\\ \frac{1}{4}\end{bmatrix},$$

$$\mathbf{c}=\begin{bmatrix}\lambda_1\\ \frac{1}{3}\\ 1\end{bmatrix},\quad \mathbf{A}=\begin{bmatrix}\lambda_1&0&0\\ \frac{1-3\lambda_2}{3}&\lambda_2&0\\ -1+3\lambda_2&2-3\lambda_2&0\end{bmatrix},\quad \mathbf{b}=\begin{bmatrix}0\\ \frac{3}{4}\\ \frac{1}{4}\end{bmatrix}.$$

The Nørsett polynomial [15] of the implicit part of the scheme corresponding to $z_0=0$ is given by $E(y)=a_4y^4+a_6y^6$ with

$$a_4=\frac{1-4\lambda_1-4\lambda_2+12\lambda_1\lambda_2}{12},\quad a_6=-\frac{(1-3\lambda_1-3\lambda_2+6\lambda_1\lambda_2)^2}{36}.$$

To obtain A-stable methods we have to assume that $a_6=0$. This leads to $\lambda_2=(1-3\lambda_1)/(3(1-2\lambda_1))$ and results in one parameter family of implicit RK methods with coefficient matrix $\mathbf{A}$ given by

$$\mathbf{A}=\begin{bmatrix}\lambda_1&0&0\\ \frac{\lambda_1}{3(1-2\lambda_1)}&\frac{1-3\lambda_1}{3(1-2\lambda_1)}&0\\ -\frac{\lambda_1}{1-2\lambda_1}&\frac{1-\lambda_1}{1-2\lambda_1}&0\end{bmatrix},$$

and the same vectors $\mathbf{c}$ and $\mathbf{b}$ as before.

We have plotted on Fig. 5.7 the area of the stability region $\mathcal{S}_\alpha$ versus λ_1 for $\alpha=\pi/2$ and $\alpha=\pi/4$. For $\alpha=\pi/2$ this area attains its maximum values approximately equal to 5.38 for $\lambda_1=0.7886866510998523$, and for $\alpha=\pi/4$ this area attains its maximum values approximately equal to 8.26 for $\lambda_1=0.7886270683133974$. The resulting methods will be denoted by IMEX-RK33$\mathcal{S}_{\pi/2}$ and IMEX-RK33$\mathcal{S}_{\pi/4}$. The points corresponding to these methods are marked by the black circles on Fig. 5.7.

Choosing $\lambda_1=(3+\sqrt{3})/6$ leads to implicit RK method for which $\lambda_1=\lambda_2$. The coefficients of this method are

$$\mathbf{c}=\begin{bmatrix}\frac{3+\sqrt{3}}{6}\\ \frac{1}{3}\\ 1\end{bmatrix},\quad \mathbf{A}=\begin{bmatrix}\frac{3+\sqrt{3}}{6}&0&0\\ -\frac{1+\sqrt{3}}{6}&\frac{3+\sqrt{3}}{6}&0\\ \frac{1+\sqrt{3}}{2}&\frac{1-\sqrt{3}}{2}&0\end{bmatrix},\quad \mathbf{b}=\begin{bmatrix}0\\ \frac{3}{4}\\ \frac{1}{4}\end{bmatrix}.$$

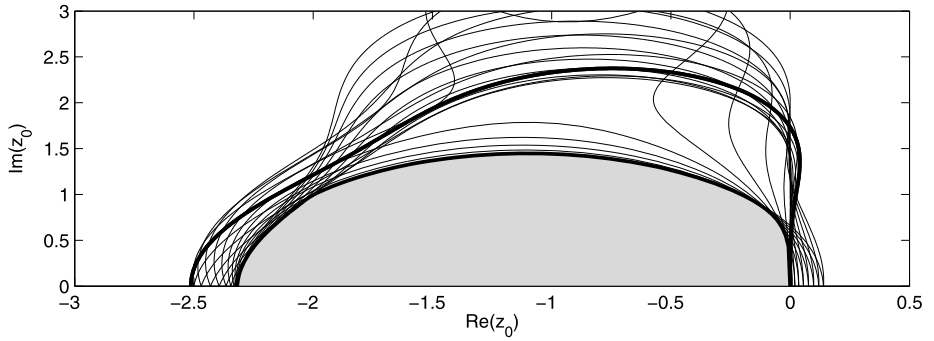

Fig. 5.8. Stability regions $\mathcal{S}_{\pi/2,y}$, $y=-2.0,-1.8,\ldots,2.0$ (thin lines), $\mathcal{S}_{\pi/2}$ (shaded region), and $\mathcal{S}_E$ (thick line) of IMEX-RK33λ.

This method will be denoted by IMEX-RK33λ. We have also plotted on Fig. 5.8 stability region $\mathcal{S}_{\pi/2}$ corresponding to $\lambda_1=\lambda_2=(3+\sqrt{3})/6$ (shaded region) and stability region $\mathcal{S}_E$ of the explicit method (thick line). We have also plotted by thin lines stability regions $\mathcal{S}_{\pi/2,y}$ for $y=-2.0,-1.8,\ldots,2.0$. The area of $\mathcal{S}_E$ is approximately equal to 9.03.

It can be verified that the second condition of (4.9) takes the form

$$\mathbf{I}-(\mathbf{I}+\gamma\overline{\mathbf{A}})^{-1}=\begin{bmatrix}0 & 0 & 0\\ \frac{\gamma}{3} & 0 & 0\\ -\frac{3\gamma+2\gamma^2}{3} & 2\gamma & 0\end{bmatrix}\geq 0.$$

This condition can be satisfied if and only if $\gamma=0$, and it follows that the explicit RK method $(\overline{\mathbf{c}},\overline{\mathbf{A}},\overline{\mathbf{b}})$ does not have SSP property.

5.4. IMEX RK schemes with $p=3$ and $s=6$

In this section we consider IMEX schemes of order $p=3$ with $s=6$ stages. We will search first for IMEX methods with maximal area of the region of absolute stability $\mathcal{S}_E$ of the explicit method $(\overline{\mathbf{c}},\overline{\mathbf{A}},\overline{\mathbf{b}})$. Solving the minimization problem (4.1) with equality constrains (4.2) corresponding to $p=3$ leads to the method which, in Matlab rational format, has the following coefficients

$$\overline{\mathbf{c}}=\begin{bmatrix}0 & \frac{83}{242} & \frac{1537}{4715} & \frac{2171}{2565} & \frac{846}{683} & \frac{667}{602}\end{bmatrix}^T,$$

$$\overline{\mathbf{A}}=\begin{bmatrix}0 & 0 & 0 & 0 & 0 & 0\\ \frac{83}{242} & 0 & 0 & 0 & 0 & 0\\ \frac{249}{15377} & \frac{307}{991} & 0 & 0 & 0 & 0\\ -\frac{239}{1758} & \frac{1080}{1687} & \frac{737}{2154} & 0 & 0 & 0\\ -\frac{220}{5231} & \frac{524}{793} & -\frac{1579}{4141} & \frac{810}{809} & 0 & 0\\ \frac{701}{7073} & -\frac{861}{1844} & \frac{1487}{1443} & \frac{809}{1433} & -\frac{135}{1132} & 0\end{bmatrix},$$

$$\overline{\mathbf{b}}=\begin{bmatrix}-\frac{181}{5045} & \frac{3288}{4885} & \frac{247}{1657} & \frac{231}{1684} & \frac{513}{3415} & -\frac{238}{3231}\end{bmatrix}^T,$$

$$\mathbf{c}=\begin{bmatrix}\frac{1247}{2772} & \frac{885}{5722} & \frac{166}{129} & \frac{1039}{866} & \frac{943}{542} & \frac{1159}{415}\end{bmatrix}^T,$$

$$\mathbf{A}=\begin{bmatrix}\frac{1247}{2772} & 0 & 0 & 0 & 0 & 0\\ -\frac{405}{1372} & \frac{1247}{2772} & 0 & 0 & 0 & 0\\ \frac{1715}{1951} & -\frac{784}{18635} & \frac{1247}{2772} & 0 & 0 & 0\\ \frac{651}{866} & -\frac{346}{1555} & \frac{4367}{19788} & \frac{1247}{2772} & 0 & 0\\ -\frac{59}{1491} & \frac{947}{1201} & \frac{235}{343} & -\frac{288}{1999} & \frac{1247}{2772} & 0\\ \frac{635}{1659} & -\frac{163}{829} & \frac{1027}{1136} & \frac{1103}{1620} & \frac{565}{988} & \frac{1247}{2772}\end{bmatrix},$$

$$\mathbf{b}=\begin{bmatrix}-\frac{181}{5045} & \frac{3288}{4885} & \frac{247}{1657} & \frac{231}{1684} & \frac{513}{3415} & -\frac{238}{3231}\end{bmatrix}^T.$$

This method will be denoted by IMEX-RK36$\mathcal{S}_E$. The coefficients of this method in double precision can be obtained from the authors. The area of stability region $\mathcal{S}_E$ of the explicit method $(\overline{\mathbf{c}},\overline{\mathbf{A}},\overline{\mathbf{b}})$ is approximately equal to 20.57, and the area of the stability region $\mathcal{S}_{\pi/2}$ is approximately equal to 8.86. The explicit method is not SSP. We have plotted on Fig. 5.9 stability

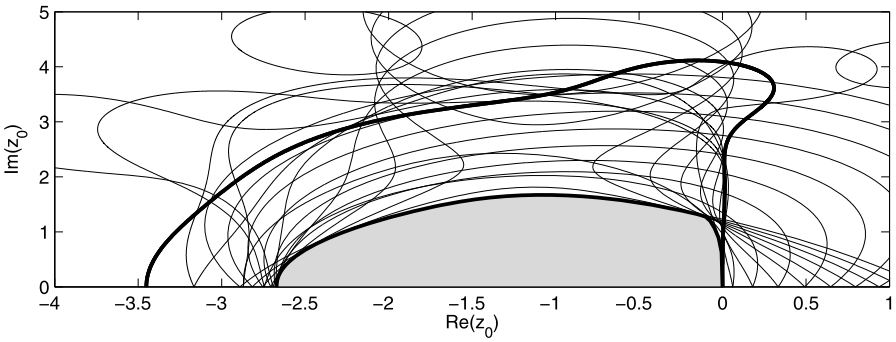

Fig. 5.9. Stability regions $\mathcal{S}_{\pi/2,y}$, $y=-6.0,-5.4,\ldots,6.0$ (thin lines), $\mathcal{S}_{\pi/2}$ (shaded region), and $\mathcal{S}_E$ (thick line) of IMEX-RK36$\mathcal{S}_E$.

region $\mathcal{S}_{\pi/2}$ (shaded region) and stability region $\mathcal{S}_E$ of the explicit method (thick line). We have also plotted by thin lines stability regions $\mathcal{S}_{\pi/2,y}$ for $y=-6.0,-5.4,\ldots,6.0$. It can be also verified that the implicit method $(\mathbf{c},\mathbf{A},\mathbf{b})$ is A-stable.

We will search next for IMEX schemes with maximal area of the region $\mathcal{S}_\alpha$ for $\alpha=\pi/2$. Solving the minimization problem (4.3) with equality constrains (4.2) we obtain the IMEX scheme with coefficients

$$\overline{\mathbf{c}}=\begin{bmatrix} 0 & \frac{243}{1945} & \frac{1231}{1834} & -\frac{223}{5417} & \frac{673}{364} & \frac{1652}{1245}\end{bmatrix}^T,$$

$$\overline{\mathbf{A}}=\begin{bmatrix} 0 & 0 & 0 & 0 & 0 & 0\\ \frac{243}{1945} & 0 & 0 & 0 & 0 & 0\\ -\frac{2988}{3461} & \frac{422}{275} & 0 & 0 & 0 & 0\\ \frac{1434}{2177} & -\frac{1522}{2231} & -\frac{71}{4019} & 0 & 0 & 0\\ -\frac{817}{10401} & -\frac{768}{1843} & \frac{631}{680} & \frac{2113}{1492} & 0 & 0\\ \frac{540}{2599} & \frac{859}{915} & \frac{1235}{1813} & -\frac{1912}{7025} & -\frac{1762}{7705} & 0\end{bmatrix},$$

$$\overline{\mathbf{b}}=\begin{bmatrix} \frac{134}{143} & -\frac{413}{3097} & \frac{830}{1311} & -\frac{430}{847} & -\frac{427}{9602} & \frac{85}{737}\end{bmatrix}^T,$$

$$\mathbf{c}=\begin{bmatrix} \frac{395}{949} & \frac{452}{977} & \frac{853}{1622} & \frac{1168}{1909} & \frac{2325}{578} & \frac{2473}{869}\end{bmatrix}^T,$$

$$\mathbf{A}=\begin{bmatrix} \frac{395}{949} & 0 & 0 & 0 & 0 & 0\\ \frac{1527}{32900} & \frac{395}{949} & 0 & 0 & 0 & 0\\ \frac{210}{5191} & \frac{165}{2384} & \frac{395}{949} & 0 & 0 & 0\\ -\frac{499}{1637} & \frac{1817}{5159} & \frac{433}{2921} & \frac{395}{949} & 0 & 0\\ \frac{2015}{1298} & \frac{1015}{1192} & \frac{1791}{1630} & \frac{251}{2423} & \frac{395}{949} & 0\\ \frac{636}{575} & \frac{139}{141} & \frac{2331}{2332} & -\frac{103}{199} & -\frac{283}{1961} & \frac{395}{949}\end{bmatrix},$$

$$\mathbf{b}=\begin{bmatrix} \frac{134}{143} & -\frac{413}{3097} & \frac{830}{1311} & -\frac{430}{847} & -\frac{427}{9602} & \frac{85}{737}\end{bmatrix}^T.$$

This method will be denoted by IMEX-RK36$\mathcal{S}_{\pi/2}$. The coefficients of this method in double precision can be obtained from the authors. The area of stability region $\mathcal{S}_E$ of the explicit method $(\overline{\mathbf{c}},\overline{\mathbf{A}},\overline{\mathbf{b}})$ is approximately equal to 10.06, and the area of the stability region $\mathcal{S}_{\pi/2}$ is approximately equal to 9.95. The explicit method is not SSP. We have plotted on Fig. 5.10 stability region $\mathcal{S}_{\pi/2}$ (shaded region) and stability region $\mathcal{S}_E$ of the explicit method (thick line). These regions are almost identical and cannot be distinguished on the Fig. 5.10, except the regions close to the imaginary axis. We have also plotted by thin lines stability regions $\mathcal{S}_{\pi/2,y}$ for $y=-6.0,-5.4,\ldots,6.0$. It can be also verified that the implicit method $(\mathbf{c},\mathbf{A},\mathbf{b})$ is A-stable.

Finally, we will search for IMEX schemes for which the explicit RK method $(\overline{\mathbf{c}},\overline{\mathbf{A}},\overline{\mathbf{b}})$ has the maximal SSP coefficient. Solving the minimization problem (4.11) with inequality constrains (4.9) and equality constrains (4.2) leads to an IMEX scheme, where the explicit methods has $\overline{s}=5$ stages. The coefficients of this scheme are given by

$$\overline{\mathbf{c}}=\begin{bmatrix} 0 & \frac{478}{1267} & \frac{873}{1157} & \frac{373}{577} & \frac{903}{1291}\end{bmatrix}^T,$$

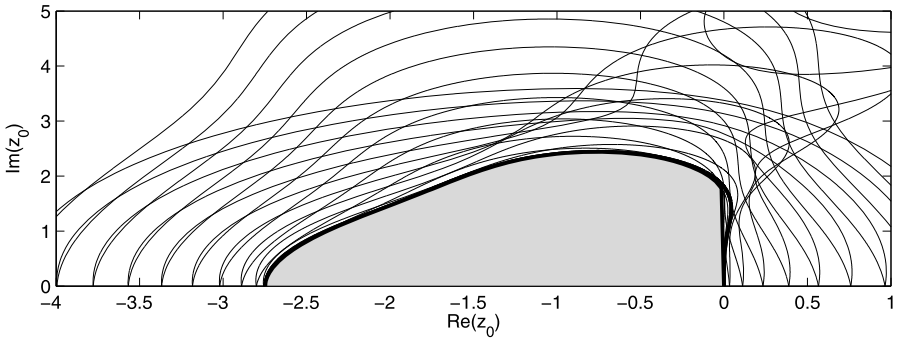

Fig. 5.10. Stability regions $\mathcal{S}_{\pi/2,y}$, $y=-6.0,-5.4,\ldots,6.0$ (thin lines), $\mathcal{S}_{\pi/2}$ (shaded region), and $\mathcal{S}_E$ (thick line) of IMEX-RK36$\mathcal{S}_{\pi/2}$.

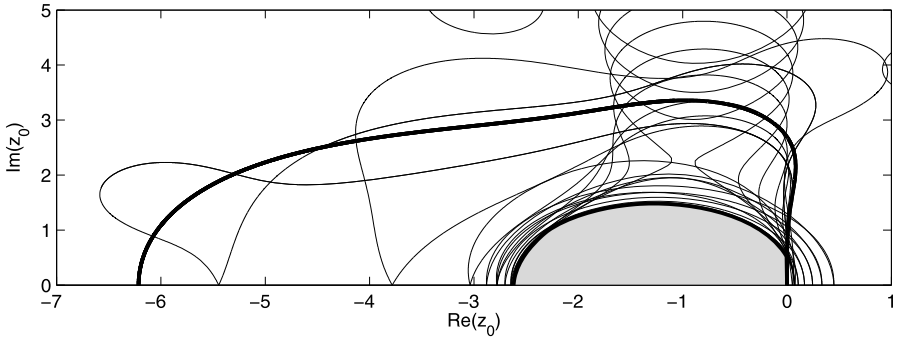

Fig. 5.11. Stability regions $\mathcal{S}_{\pi/2,y}$, $y=-6.0,-5.4,\ldots,6.0$ (thin lines), $\mathcal{S}_{\pi/2}$ (shaded region), and $\mathcal{S}_E$ (thick line) of IMEX-RK36SSP.

$$\overline{\mathbf{A}}=\begin{bmatrix} 0 & 0 & 0 & 0 & 0\\ \frac{478}{1267} & 0 & 0 & 0 & 0\\ \frac{478}{1267} & \frac{478}{1267} & 0 & 0 & 0\\ \frac{476}{2209} & \frac{476}{2209} & \frac{476}{2209} & 0 & 0\\ \frac{762}{3697} & \frac{637}{4843} & \frac{637}{4843} & \frac{1498}{6505} & 0 \end{bmatrix},$$

$$\overline{\mathbf{b}}=\begin{bmatrix} \frac{159}{707} & \frac{210}{1793} & \frac{213}{1819} & \frac{605}{2951} & \frac{397}{1182} \end{bmatrix}^T,$$

$$\mathbf{c}=\begin{bmatrix} \frac{1934}{4175} & 0 & \frac{478}{1267} & \frac{873}{1157} & \frac{373}{577} & \frac{903}{1291} \end{bmatrix}^T,$$

$$\mathbf{A}=\begin{bmatrix} \frac{1934}{4175} & 0 & 0 & 0 & 0 & 0\\ -\frac{1934}{4175} & \frac{1934}{4175} & 0 & 0 & 0 & 0\\ \frac{461}{1770} & -\frac{203}{586} & \frac{1934}{4175} & 0 & 0 & 0\\ -\frac{876}{545} & \frac{889}{437} & -\frac{478}{3523} & \frac{1934}{4175} & 0 & 0\\ \frac{1081}{1934} & \frac{19144}{78703} & -\frac{1597}{1624} & \frac{391}{1073} & \frac{1934}{4175} & 0\\ \frac{339}{773} & \frac{300}{9379} & -\frac{353}{1743} & -\frac{213}{1154} & \frac{244}{1597} & \frac{1934}{4175} \end{bmatrix},$$

$$\mathbf{b}=\begin{bmatrix} 0 & \frac{431}{1916} & \frac{671}{5743} & \frac{327}{2791} & \frac{385}{1868} & \frac{691}{2063} \end{bmatrix}^T.$$

This method will be denoted by IMEX-RK36SSP. The coefficients of this method in double precision can be obtained from the authors. The area of stability region $\mathcal{S}_E$ of the explicit method $(\overline{\mathbf{c}},\overline{\mathbf{A}},\overline{\mathbf{b}})$ is approximately equal to 33.03, and the area of the stability region $\mathcal{S}_{\pi/2}$ is approximately equal to 6.19. The explicit method $(\overline{\mathbf{c}},\overline{\mathbf{A}},\overline{\mathbf{b}})$ has SSP property with the effective SSP coefficient $\mathcal{C}_{eff}=\mathcal{C}/\overline{s}=0.530$. We have plotted on Fig. 5.11 stability region $\mathcal{S}_{\pi/2}$ (shaded region) and stability region $\mathcal{S}_E$ of the explicit method (thick line). We have also plotted by thin lines stability regions $\mathcal{S}_{\pi/2,y}$ for $y=-6.0,-5.4,\ldots,6.0$. The implicit method $(\mathbf{c},\mathbf{A},\mathbf{b})$ is not A-stable.

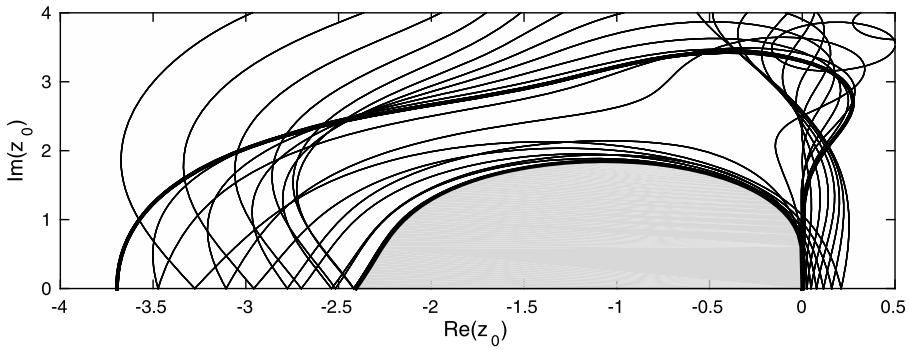

Fig. 5.12. Stability regions $\mathcal{S}_{\pi/2,y}$, $y = -6.0, -5.4, \ldots, 6.0$ (thin lines), $\mathcal{S}_{\pi/2}$ (shaded region), and $\mathcal{S}_E$ (thick line) of IMEX-RK48$\mathcal{S}_E$.

5.5. IMEX RK schemes with $p = 4$ and $s = 8$

In this section we consider IMEX schemes of order $p = 4$ with $s = 8$ stages. We will search first for IMEX methods with maximal area of the region of absolute stability $\mathcal{S}_E$ of the explicit method $(\overline{\mathbf{c}}, \overline{\mathbf{A}}, \overline{\mathbf{b}})$. Solving the minimization problem (4.1) with equality constrains (4.2) corresponding to $p = 4$ leads to the method which, in Matlab rational format, has the following coefficients

$$\overline{\mathbf{c}} = \begin{bmatrix} 0 & \frac{326}{1379} & \frac{1749}{7034} & \frac{1966}{2349} & \frac{792}{571} & \frac{1123}{1129} & \frac{1729}{2381} & \frac{561}{397} \end{bmatrix}^T,$$

$$\overline{\mathbf{A}} = \begin{bmatrix} 0 & 0 & 0 & 0 & 0 & 0 & 0 & 0 \\ \frac{326}{1379} & 0 & 0 & 0 & 0 & 0 & 0 & 0 \\ -\frac{1450}{19477} & \frac{1031}{3191} & 0 & 0 & 0 & 0 & 0 & 0 \\ \frac{128}{15375} & -\frac{69}{1555} & \frac{873}{1000} & 0 & 0 & 0 & 0 & 0 \\ \frac{377}{7459} & \frac{959}{1044} & -\frac{119}{10006} & \frac{943}{2194} & 0 & 0 & 0 & 0 \\ \frac{39}{10744} & \frac{181}{216294} & \frac{254}{1269} & \frac{573}{832} & \frac{179}{1766} & 0 & 0 & 0 \\ \frac{113}{5084} & \frac{902}{2137} & \frac{127}{6960} & \frac{57}{7948} & \frac{713}{10786} & \frac{492}{2585} & 0 & 0 \\ -\frac{372}{3299} & \frac{195}{8234} & \frac{581}{1495} & \frac{569}{622} & \frac{207}{2612} & \frac{169}{2983} & \frac{255}{4057} & 0 \end{bmatrix},$$

$$\overline{\mathbf{b}} = \begin{bmatrix} \frac{43}{142610} & \frac{485}{3662} & \frac{849}{1915} & \frac{502}{1401} & -\frac{73}{2952} & \frac{318}{3289} & -\frac{339}{41053} & \frac{47}{24734} \end{bmatrix}^T,$$

$$\mathbf{c} = \begin{bmatrix} \frac{1095}{3943} & \frac{200}{847} & \frac{142}{571} & \frac{763}{911} & \frac{694}{501} & \frac{5197}{5196} & \frac{766}{953} & \frac{8612}{6615} \end{bmatrix}^T,$$

$$\mathbf{A} = \begin{bmatrix} \frac{1095}{3943} & 0 & 0 & 0 & 0 & 0 & 0 & 0 \\ -\frac{1159}{27874} & \frac{1095}{3943} & 0 & 0 & 0 & 0 & 0 & 0 \\ \frac{91}{1265} & -\frac{116}{1149} & \frac{1095}{3943} & 0 & 0 & 0 & 0 & 0 \\ -\frac{2538}{5135} & -\frac{283}{674} & \frac{1897}{1287} & \frac{1095}{3943} & 0 & 0 & 0 & 0 \\ \frac{3545}{2933} & \frac{1243}{331} & -\frac{859}{554} & -\frac{196}{85} & \frac{1095}{3943} & 0 & 0 & 0 \\ \frac{2729}{1518} & \frac{1471}{425} & -\frac{1100}{317} & -\frac{3138}{2975} & -\frac{77}{6619} & \frac{1095}{3943} & 0 & 0 \\ \frac{125}{3524} & -\frac{1151}{4318} & \frac{238}{369} & -\frac{637}{792} & -\frac{971}{680} & \frac{1341}{572} & \frac{1095}{3943} & 0 \\ \frac{681}{191} & \frac{2337}{281} & -\frac{3396}{409} & -\frac{1122}{523} & \frac{2521}{872} & -\frac{4265}{788} & \frac{4247}{2011} & \frac{1095}{3943} \end{bmatrix},$$

$$\mathbf{b} = \begin{bmatrix} \frac{43}{142610} & \frac{485}{3662} & \frac{849}{1915} & \frac{502}{1401} & -\frac{73}{2952} & \frac{318}{3289} & -\frac{339}{41053} & \frac{47}{24734} \end{bmatrix}^T.$$

This method will be denoted by IMEX-RK48$\mathcal{S}_E$. The coefficients of this method in double precision can be obtained from the authors. The area of stability region $\mathcal{S}_E$ of the explicit method $(\overline{\mathbf{c}}, \overline{\mathbf{A}}, \overline{\mathbf{b}})$ is approximately equal to 19.36, and the area of the stability region $\mathcal{S}_{\pi/2}$ is approximately equal to 7.06. The explicit method is not SSP. We have plotted on Fig. 5.12 stability region $\mathcal{S}_{\pi/2}$ (shaded region) and stability region $\mathcal{S}_E$ of the explicit method (thick line). We have also plotted by thin lines stability regions $\mathcal{S}_{\pi/2,y}$ for $y = -6.0, -5.4, \ldots, 6.0$. It can be also verified that the implicit method $(\mathbf{c}, \mathbf{A}, \mathbf{b})$ is A-stable.

We will search next for IMEX schemes with maximal area of the region $\mathcal{S}_\alpha$ for $\alpha = \pi/2$. Solving the minimization problem (4.3) with equality constrains (4.2) we obtain the IMEX scheme which, in Matlab rational format, has the following coefficients

$$\overline{\mathbf{c}} = \begin{bmatrix} 0 & \frac{1378}{5483} & \frac{132}{2885} & \frac{16115}{29712} & \frac{389}{670} & \frac{327}{200} & \frac{992}{383} & \frac{2648}{695} \end{bmatrix}^T,$$

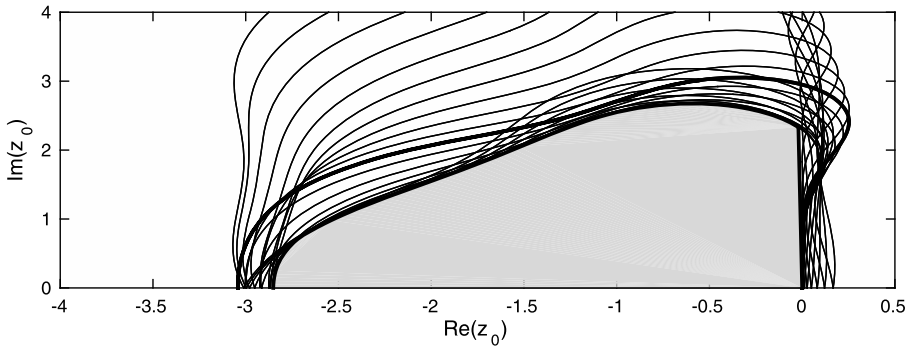

Fig. 5.13. Stability regions $\mathcal{S}_{\pi/2,y}$, $y = -6.0, -5.4, \ldots, 6.0$ (thin lines), $\mathcal{S}_{\pi/2}$ (shaded region), and $\mathcal{S}_E$ (thick line) of IMEX-RK48$\mathcal{S}_{\pi/2}$.

$$\overline{\mathbf{A}} = \begin{bmatrix} 0 & 0 & 0 & 0 & 0 & 0 & 0 & 0 \\ \frac{1378}{5483} & 0 & 0 & 0 & 0 & 0 & 0 & 0 \\ -\frac{41}{24173} & \frac{361}{7608} & 0 & 0 & 0 & 0 & 0 & 0 \\ \frac{52}{10845} & \frac{1975}{3728} & \frac{64}{8201} & 0 & 0 & 0 & & \\ \frac{7}{7667} & -\frac{8}{2993} & \frac{573}{2038} & \frac{653}{2168} & 0 & 0 & 0 & 0 \\ -\frac{29}{18805} & -\frac{139}{16295} & \frac{508}{17301} & \frac{1341}{2486} & \frac{917}{852} & 0 & 0 & 0 \\ \frac{153}{1705} & \frac{625}{364} & \frac{543}{3089} & \frac{595}{5118} & \frac{511}{5378} & \frac{275}{694} & 0 & 0 \\ \frac{1546}{787} & \frac{613}{2040} & \frac{61}{3045} & \frac{460}{909} & \frac{398}{5743} & \frac{594}{863} & \frac{467}{1786} & 0 \end{bmatrix},$$

$$\overline{\mathbf{b}} = \begin{bmatrix} 0 & 0 & \frac{1265}{5853} & \frac{5}{3733} & \frac{3055}{4101} & \frac{591}{13898} & -\frac{152}{30203} & \frac{25}{249031} \end{bmatrix}^T,$$

$$\mathbf{c} = \begin{bmatrix} \frac{217}{849} & \frac{469}{1878} & \frac{132}{2885} & \frac{16115}{29712} & \frac{389}{670} & \frac{327}{200} & \frac{992}{383} & \frac{2648}{695} \end{bmatrix}^T,$$

$$\mathbf{A} = \begin{bmatrix} \frac{217}{849} & 0 & 0 & 0 & 0 & 0 & 0 & 0 \\ -\frac{95}{16208} & \frac{217}{849} & 0 & 0 & 0 & 0 & 0 & 0 \\ \frac{620}{1539} & -\frac{1264}{2063} & \frac{217}{849} & 0 & 0 & 0 & 0 & 0 \\ -\frac{762}{2513} & \frac{1357}{3196} & \frac{241}{1457} & \frac{217}{849} & 0 & 0 & 0 & 0 \\ -\frac{861}{5003} & \frac{963}{1726} & \frac{56}{1329} & -\frac{443}{4302} & \frac{217}{849} & 0 & 0 & 0 \\ \frac{2822}{3033} & -\frac{2477}{316} & \frac{2407}{601} & \frac{3079}{404} & -\frac{5392}{1615} & \frac{217}{849} & 0 & 0 \\ -\frac{1119}{2579} & -\frac{1583}{160} & \frac{5987}{628} & -\frac{3054}{745} & \frac{520}{99} & \frac{2337}{1183} & \frac{217}{849} & 0 \\ -\frac{2282}{1087} & -\frac{1880}{791} & \frac{9181}{955} & \frac{6049}{741} & -\frac{5507}{556} & -\frac{1559}{274} & \frac{2965}{507} & \frac{217}{849} \end{bmatrix},$$

$$\mathbf{b} = \begin{bmatrix} 0 & 0 & \frac{1265}{5853} & \frac{5}{3733} & \frac{3055}{4101} & \frac{591}{13898} & -\frac{152}{30203} & \frac{25}{249031} \end{bmatrix}^T.$$

This method will be denoted by IMEX-RK48$\mathcal{S}_{\pi/2}$. The coefficients of this method in double precision can be obtained from the authors. The area of stability region $\mathcal{S}_E$ of the explicit method $(\overline{\mathbf{c}}, \overline{\mathbf{A}}, \overline{\mathbf{b}})$ is approximately equal to 13.87, and the area of the stability region $\mathcal{S}_{\pi/2}$ is approximately equal to 11.02. The explicit method is not SSP. We have plotted on Fig. 5.13 stability region $\mathcal{S}_{\pi/2}$ (shaded region) and stability region $\mathcal{S}_E$ of the explicit method (thick line). We have also plotted by thin lines stability regions $\mathcal{S}_{\pi/2,y}$ for $y = -6.0, -5.4, \ldots, 6.0$. It can be also verified that the implicit method $(\mathbf{c}, \mathbf{A}, \mathbf{b})$ is A-stable.

As in previous sections we will search next for IMEX schemes for which the explicit RK method $(\overline{\mathbf{c}}, \overline{\mathbf{A}}, \overline{\mathbf{b}})$ has the maximal SSP coefficient. Solving the minimization problem (4.11) with inequality constrains (4.9) and equality constrains (4.2) leads to an IMEX scheme with coefficients given by

$$\overline{\mathbf{c}} = \begin{bmatrix} 0 & 0 & \frac{641}{1353} & \frac{275}{588} & \frac{1268}{703} & \frac{521}{570} & \frac{799}{171} & \frac{879}{1063} \end{bmatrix}^T,$$

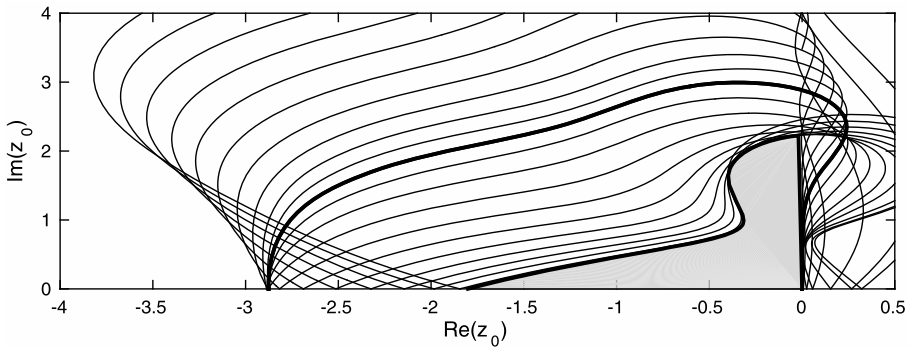

Fig. 5.14. Stability regions $\mathcal{S}_{\pi/2,y}$, $y=-6.0,-5.4,\ldots,6.0$ (thin lines), $\mathcal{S}_{\pi/2}$ (shaded region), and $\mathcal{S}_E$ (thick line) of IMEX-RK48SSP.

$$\overline{\mathbf{A}}=\begin{bmatrix} 0 & 0 & 0 & 0 & 0 & 0 & 0 & 0\\ 0 & 0 & 0 & 0 & 0 & 0 & 0 & 0\\ 0 & \frac{966}{2039} & 0 & 0 & 0 & 0 & 0 & 0\\ 0 & \frac{199}{5291} & \frac{735}{1709} & 0 & 0 & 0 & 0 & 0\\ 0 & \frac{306}{4373} & \frac{533}{1060} & \frac{773}{628} & 0 & 0 & 0 & 0\\ 0 & \frac{61}{10399} & \frac{552}{8267} & \frac{881}{1054} & \frac{52}{9395} & 0 & 0 & 0\\ \frac{184}{2869} & \frac{141}{3059} & \frac{826}{1929} & \frac{1567}{757} & \frac{1754}{977} & \frac{161}{599} & 0 & 0\\ 0 & \frac{27}{359} & \frac{227}{2338} & \frac{53}{557} & \frac{569}{4644} & \frac{859}{1966} & 0 & 0 \end{bmatrix},$$

$$\overline{\mathbf{b}}=\begin{bmatrix} 0 & \frac{277}{1720} & \frac{385}{1314} & \frac{587}{1885} & \frac{31}{18247} & \frac{665}{2906} & 0 & \frac{23}{5731} \end{bmatrix}^T,$$

$$\mathbf{c}=\begin{bmatrix} \frac{1026}{3919} & 0 & \frac{641}{1353} & \frac{275}{588} & \frac{1268}{703} & \frac{521}{570} & \frac{3127}{657} & \frac{879}{1063} \end{bmatrix}^T,$$

$$\mathbf{A}=\begin{bmatrix} \frac{1026}{3919} & 0 & 0 & 0 & 0 & 0 & 0 & 0\\ -\frac{1148}{4385} & \frac{1026}{3919} & 0 & 0 & 0 & 0 & 0 & 0\\ -\frac{1165}{2683} & \frac{904}{1399} & \frac{1026}{3919} & 0 & 0 & 0 & 0 & 0\\ \frac{1480}{2439} & -\frac{1469}{4070} & -\frac{121}{3026} & \frac{1026}{3919} & 0 & 0 & 0 & 0\\ -\frac{2788}{397} & \frac{2069}{294} & \frac{722}{339} & -\frac{411}{682} & \frac{1026}{3919} & 0 & 0 & 0\\ -\frac{165}{12667} & \frac{105}{671} & \frac{133}{500} & \frac{1307}{5430} & \frac{55}{26474} & \frac{1026}{3919} & 0 & 0\\ \frac{837}{1003} & \frac{629}{1976} & \frac{1195}{149} & -\frac{5209}{618} & \frac{1045}{1459} & \frac{2767}{911} & \frac{1026}{3919} & 0\\ -\frac{752}{647} & -\frac{771}{2338} & \frac{3197}{469} & \frac{2313}{586} & -\frac{2267}{2341} & -\frac{2128}{275} & 0 & \frac{1026}{3919} \end{bmatrix},$$

$$\mathbf{b}=\begin{bmatrix} 0 & \frac{277}{1720} & \frac{385}{1314} & \frac{587}{1885} & \frac{31}{18247} & \frac{665}{2906} & 0 & \frac{23}{5731} \end{bmatrix}^T.$$

This method will be denoted by IMEX-RK48SSP. The coefficients of this method in double precision can be obtained from the authors. The area of stability region $\mathcal{S}_E$ of the explicit method $(\overline{\mathbf{c}},\overline{\mathbf{A}},\overline{\mathbf{b}})$ is approximately equal to 12.90, and the area of the stability region $\mathcal{S}_{\pi/2}$ is approximately equal to 2.64. The explicit method $(\overline{\mathbf{c}},\overline{\mathbf{A}},\overline{\mathbf{b}})$ has SSP property with the effective SSP coefficient $\mathcal{C}_{eff}=\mathcal{C}/\overline{s}=0.023$. We have plotted on Fig. 5.14 stability region $\mathcal{S}_{\pi/2}$ (shaded region) and stability region $\mathcal{S}_E$ of the explicit method (thick line). We have also plotted by thin lines stability regions $\mathcal{S}_{\pi/2,y}$ for $y=-6.0,-5.4,\ldots,6.0$. The implicit method $(\mathbf{c},\mathbf{A},\mathbf{b})$ is not A-stable.

6. Numerical experiments

6.1. Van der Pol oscillator

As first test problem for our numerical experiments we consider the van der Pol oscillator (see VDPOL problem in [15])

$$\begin{cases} y_1'=y_2,\\ y_2'=\big((1-y_1^2)y_2-y_1\big)/\varepsilon, \end{cases} \tag{6.1}$$

$t\in[0,T]$, with initial conditions

$$y_1(0)=2,\quad y_2(0)=-\frac{2}{3}+\frac{10}{81}\varepsilon-\frac{292}{2187}\varepsilon^2-\frac{1814}{19683}\varepsilon^3+O(\varepsilon^4), \tag{6.2}$$

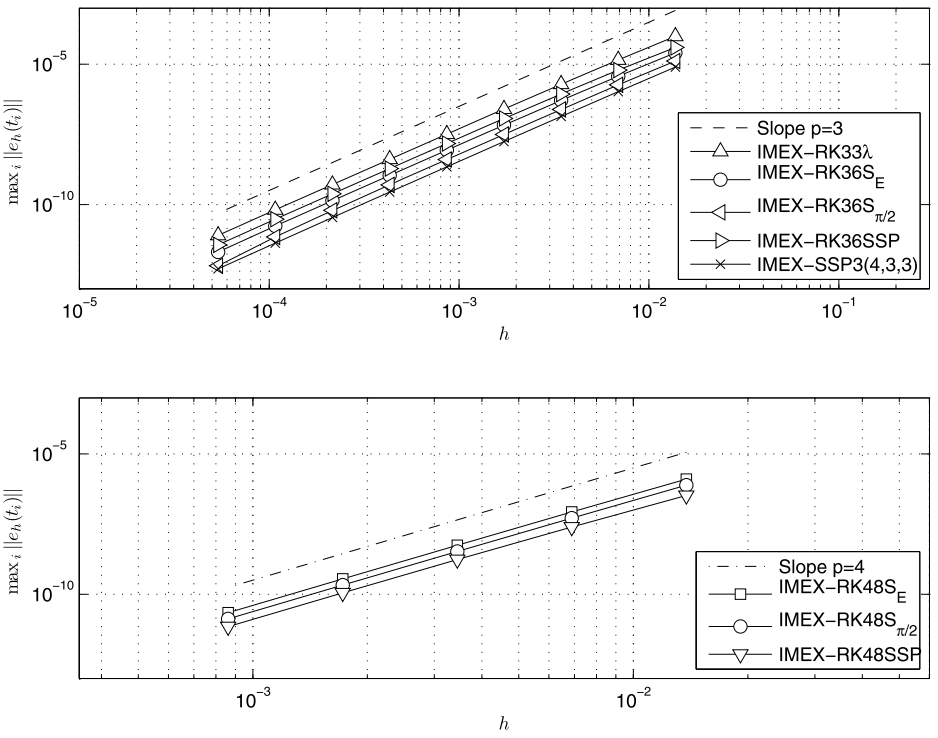

Fig. 6.1. Error versus stepsize (double logarithmic scale plot) for IMEX RK methods of order $p = 3$ and $p = 4$ on the van der Pol problem (6.1)–(6.2) with $\varepsilon = 10^{-1}$.

with a stiffness parameter ε. We write the system (6.1) as (1.1), by setting

$$f(y) = \begin{bmatrix} y_2 \\ 0 \end{bmatrix} \quad \text{and} \quad g(y) = \begin{bmatrix} 0 \\ ((1-y_1^2)y_2 - y_1)/\varepsilon \end{bmatrix}.$$

We have implemented the methods constructed in this paper with a fixed stepsize h, and observed the order of convergence of the numerical approximations to the slowly varying parts of the solution, where the problem is stiff for small values of the parameter ε. We compare the numerical results for the solution all over the integration grid with a reference solution computed by the Matlab function `ode15s` with very tight tolerances $atol = 10^{-16}$ and $rtol = 10^{-14}$. The errors are measured in the $||\cdot||_\infty$ norm.

The observed experimental orders have been reported in Fig. 6.1–6.3 for $T = 0.55139$ (compare [15]) and for different values of ε. In particular Figs. 6.1 and 6.2 show that the methods of order $p = 3$ and $p = 4$ constructed in Sections 5.3–5.5 match the theoretical predictions and preserve the expected order when applied to the van der Pol problem (6.1)–(6.2) with values of the parameter $\varepsilon = 10^{-1}$ and $\varepsilon = 10^{-3}$ which correspond to nonstiff and mildly stiff problems, respectively. Similar pictures, obtained for methods of order $p = 2$ constructed in Sections 5.1 and 5.2, are not reported here. Fig. 6.3 shows that the IMEX RK methods can suffer from the well known order reduction phenomenon when the problem (6.1)–(6.2) is stiff, but the order is still preserved for small values of the stepsize h. To the aim of comparison we also reported in Fig. 6.1, 6.2 and 6.3 the numerical solution obtained by the method IMEX-SSP3(4,3,3) derived in [27]. The construction of IMEX general linear methods with high stage order which overcome the order reduction issue is treated by the authors in [8].

6.2. Schnackenberg's model

Following [16] our next test model for the IMEX schemes is the system of reaction–diffusion equations in two space variables

$$\begin{cases} \dfrac{\partial u}{\partial t} = D_1\left(\dfrac{\partial^2 u}{\partial x^2} + \dfrac{\partial^2 u}{\partial y^2}\right) + \kappa\left(a - u + u^2 v\right), \\ \dfrac{\partial v}{\partial t} = D_2\left(\dfrac{\partial^2 v}{\partial x^2} + \dfrac{\partial^2 v}{\partial y^2}\right) + \kappa\left(b - u^2 v\right), \end{cases} \tag{6.3}$$

$0 \le x, y \le 1$, $t \ge 0$, with initial conditions

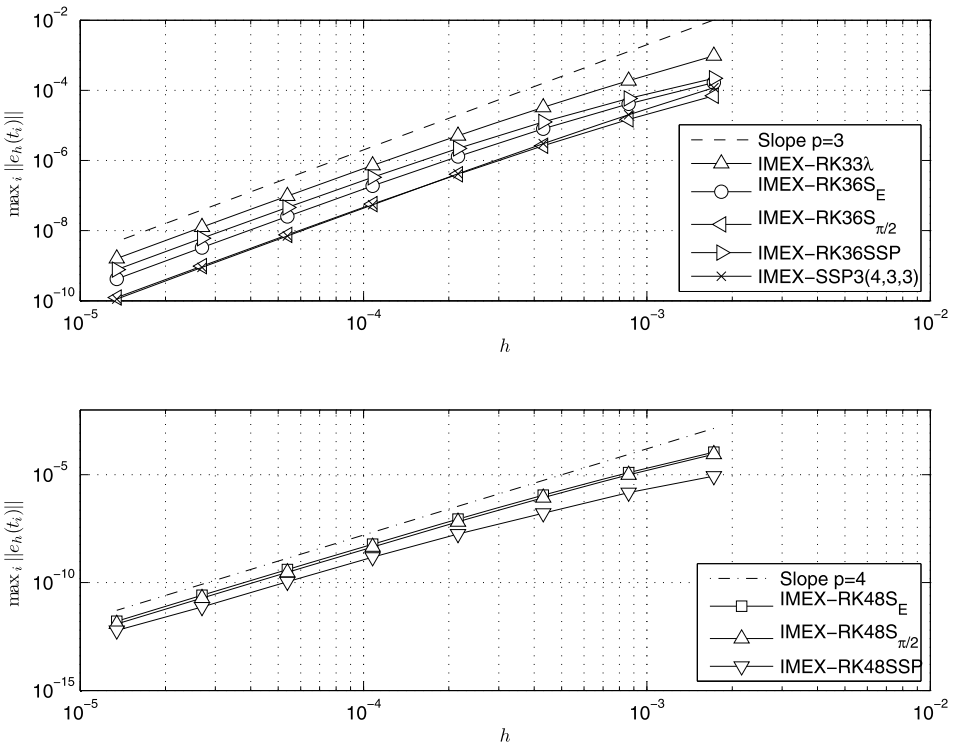

Fig. 6.2. Error versus stepsize (double logarithmic scale plot) for IMEX RK methods of order $p = 3$ and $p = 4$ on the van der Pol problem (6.1)–(6.2) with $\varepsilon = 10^{-3}$.

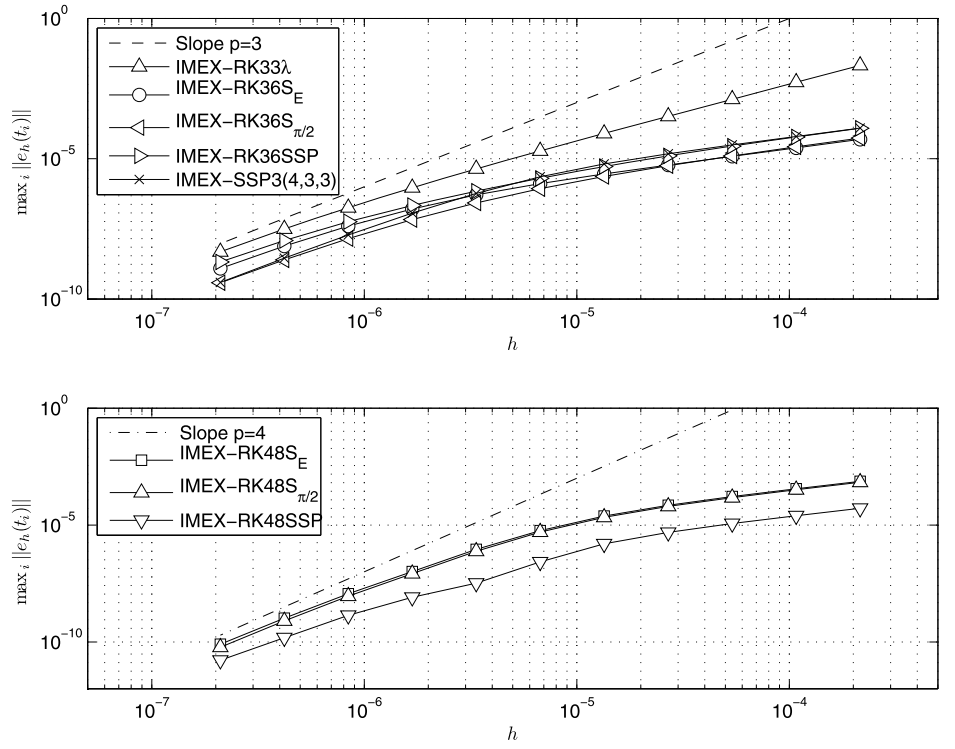

Fig. 6.3. Error versus stepsize (double logarithmic scale plot) for IMEX RK methods of order $p = 3$ and $p = 4$ on the van der Pol problem (6.1)–(6.2) with $\varepsilon = 10^{-6}$.

Table 6.1
L_∞-norm of errors and observed orders of convergence p for IMEX RK methods applied to the discretization (6.4) of reaction–diffusion equations (6.3) by second order finite differences in space variables for the diffusion terms, with $N = M = 21$.

h	IMEX-RK22Lm		IMEX-RK33λ		IMEX-RK36$\mathcal{S}_{\pi/2}$		IMEX-RK48SSP	
	$\|\text{error}\|_\infty$	p	$\|\text{error}\|_\infty$	p	$\|\text{error}\|_\infty$	p	$\|\text{error}\|_\infty$	p
1.0000e−03	1.35e−01		6.31e−02		9.59e−02		4.08e−03	
5.0000e−04	2.61e−02	2.37	8.99e−03	2.81	2.15e−02	2.15	3.14e−04	3.70
2.5000e−04	5.63e−03	2.21	1.36e−03	2.72	3.71e−03	2.54	2.26e−05	3.80
1.2500e−04	1.30e−03	2.11	1.98e−04	2.78	5.53e−04	2.75	1.53e−06	3.89
6.2500e−05	3.12e−04	2.06	2.72e−05	2.86	7.58e−05	2.87	9.93e−08	3.94
3.1250e−05	7.64e−05	2.03	3.59e−06	2.92	9.93e−06	2.93	8.23e−09	3.59

$$u(x,y,0) = a + b + 10^{-3}\exp\left(-100\left(\left(x-\tfrac{1}{2}\right)^2 + \left(y-\tfrac{1}{3}\right)^2\right)\right),$$
$$v(x,y,0) = \tfrac{b}{(a+b)^2},$$

and the homogeneous Neumann boundary conditions

$$\frac{\partial u}{\partial x}(0,y,t) = \frac{\partial u}{\partial x}(1,y,t) = 0, \quad \frac{\partial u}{\partial y}(x,0,t) = \frac{\partial u}{\partial y}(x,1,t) = 0,$$
$$\frac{\partial v}{\partial x}(0,y,t) = \frac{\partial v}{\partial x}(1,y,t) = 0, \quad \frac{\partial v}{\partial y}(x,0,t) = \frac{\partial v}{\partial y}(x,1,t) = 0.$$

The parameter values are $a = 0.1305$, $b = 0.7695$, $D_1 = 0.05$, $D_2 = 1$, $\kappa = 100$. This model is due to Schnackenberg [29] and it is related to the Gray-Scott model for pattern formation described in [28]. As observed in [16], it is stiff already on rather coarse grids, due to relatively large diffusion coefficients.

The system (6.3) was discretized on the uniform grids in space variables x and y, $x_i = (i-1)\Delta x$, for $i = 1, 2, \ldots, N$, $(N-1)\Delta x = 1$, $y_j = (j-1)\Delta y$, for $j = 1, 2, \ldots, M$, $(M-1)\Delta y = 1$, using standard second order finite differences in space for the diffusion terms. This leads to the system of ODEs of dimension $2NM$ for the unknown functions $u_{ij}(t) \approx u(x_i, y_j, t)$ and $v_{ij}(t) \approx v(x_i, y_j, t)$ of the form

$$\begin{cases} u'_{ij} &= D_1\left(\dfrac{u_{i+1,j} - 2u_{ij} + u_{i-1,j}}{\Delta x^2} + \dfrac{u_{i,j+1} - 2u_{ij} + u_{i-1,j}}{\Delta y^2}\right) - u_{ij}v_{ij}^2 + \gamma(1 - u_{ij}), \\ v'_{ij} &= D_2\left(\dfrac{v_{i+1,j} - 2v_{ij} + v_{i-1,j}}{\Delta x^2} + \dfrac{v_{i,j+1} - 2v_{ij} + v_{i-1,j}}{\Delta y^2}\right) + u_{ij}v_{ij}^2 - (\gamma + \kappa)v_{ij}, \end{cases} \tag{6.4}$$

$i = 1, 2, \ldots, N$, $j = 1, 2, \ldots, M$, with initial conditions

$$u_{ij}(0) = a + b + 10^{-3}\exp\left(-100\left(\left(x_i - \frac{1}{2}\right)^2 + \left(y_j - \frac{1}{3}\right)^2\right)\right),$$
$$v_{ij}(0) = \frac{b}{(a+b)^2},$$

$i = 1, 2, \ldots, N$, $j = 1, 2, \ldots, M$. Because of the boundary conditions we have

$$u_{0,j} = u_{2,j}, \quad u_{N+1,j} = u_{N-1,j}, \quad u_{i,0} = u_{i,2}, \quad u_{i,M+1} = u_{i,M-1},$$
$$v_{0,j} = v_{2,j}, \quad v_{N+1,j} = v_{N-1,j}, \quad v_{i,0} = v_{i,2}, \quad v_{i,M+1} = v_{i,M-1}.$$

This system of ODEs (6.4) was then solved by IMEX schemes IMEX-RK22Lm, IMEX-RK33λ, IMEX-RK36$\mathcal{S}_{\pi/2}$ and IMEX-RK48SSP, where the diffusion terms were treated by implicit method and the reaction terms by the explicit methods. A selection of the results of numerical experiments are presented in Table 6.1, where the maximum errors all over the integration grid has been reported. We can see that all the considered methods achieve the expected order of convergence.

6.3. One-dimensional shallow water model

We now consider a one-dimensional model of shallow water flow (compare [22,27]):

$$\begin{cases} \dfrac{\partial}{\partial t}h + \dfrac{\partial}{\partial x}(hv) = 0, \\ \dfrac{\partial}{\partial t}(hv) + \dfrac{\partial}{\partial x}\left(h^2 + \dfrac{1}{2}h^2\right) = \dfrac{1}{\varepsilon}\left(\dfrac{h^2}{2} - hv\right), \end{cases} \tag{6.5}$$

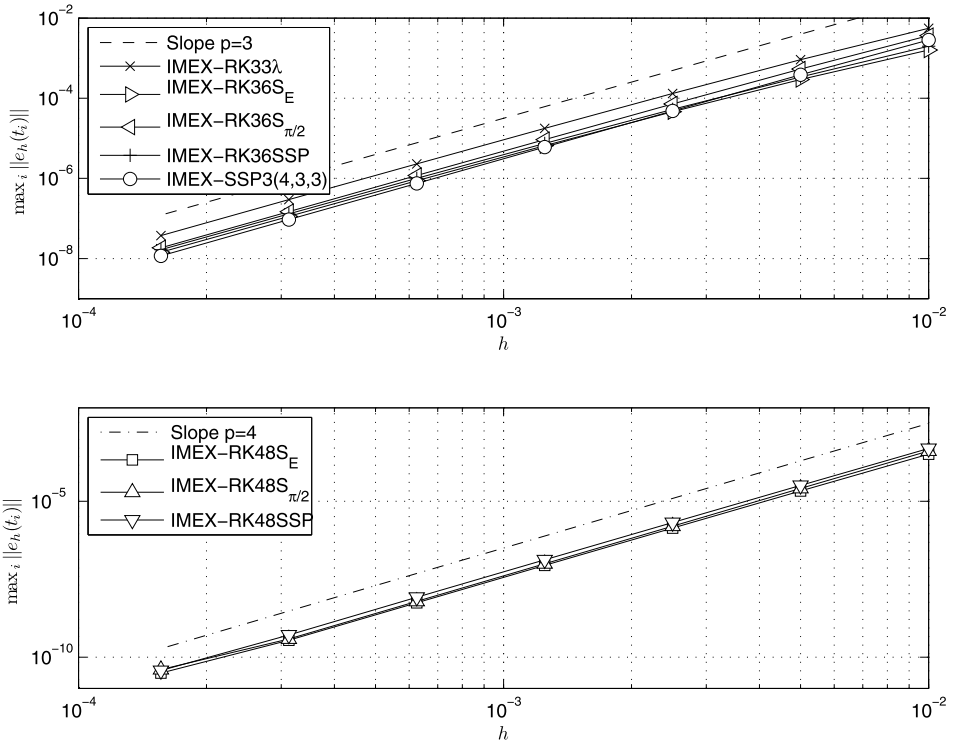

Fig. 6.4. Error versus stepsize (double logarithmic scale plot) for IMEX RK methods of order $p = 3$ and $p = 4$ on the one-dimensional shallow water problem (6.5) with boundary conditions (6.6) and $\varepsilon = 10^{-2}$.

where h is the water height with respect to the bottom and hv is the flux of the velocity field. We use periodic boundary conditions and initial conditions at $t_0 = 0$

$$h(0,x) = 1 + \frac{1}{5}\sin(8\pi x), \quad hv(0,x) = \frac{1}{2}h(0,x)^2, \tag{6.6}$$

with $x \in [0,1]$. For this problem the space derivative was discretized by a fifth order finite difference weighted essentially non-oscillatory (WENO) scheme following the implementation described in [30]. The results at $t = 0.5$ obtained by the numerical methods of order $p = 3$ and $p = 4$ constructed in Sections 5.3–5.5 are reported in Figs. 6.4 and 6.5, where the maximum error all over the integration grid is computed with respect to a reference solution computed by the Matlab function `ode15s` with very tight tolerances $atol = 10^{-16}$ and $rtol = 10^{-14}$. The errors are measured in the $||\cdot||_\infty$ norm. Again, to the aim of comparison we also reported the numerical results obtained by the method IMEX-SSP3(4,3,3) derived in [27].

All numerical experiments reported in this paper were performed in a fixed stepsize environment, and they illustrate that the IMEX schemes constructed in this paper achieve the expected order of accuracy for some range of stepsizes. To compare these methods to other schemes constructed in the literature on the subject it would be also of interest to perform similar experiments for variable stepsizes. However, this would require the construction of accurate and reliable error estimators for large and small stepsizes and the development of appropriate step size changing strategies for IMEX methods. The analysis of these implementation issues requires different tools than those employed in this paper, which deals with the construction of IMEX RK methods with desirable stability properties. These implementation topics, in the context of IMEX RK methods, and in a more general context of IMEX general linear methods, will be investigated in a future work.

7. Concluding remarks

We considered the class of IMEX RK methods and we investigated the construction of good methods from three different points of view. In particular we derived IMEX RK methods of order $p = 2$, $p = 3$ and $p = 4$ by maximizing:

- the area of the region of absolute stability $\mathcal{S}_E$ of explicit RK method (2.2);
- the area of the stability region S_α for $\alpha = \pi/2$ and $\alpha = \pi/4$;
- the SSP coefficient of the explicit RK method.

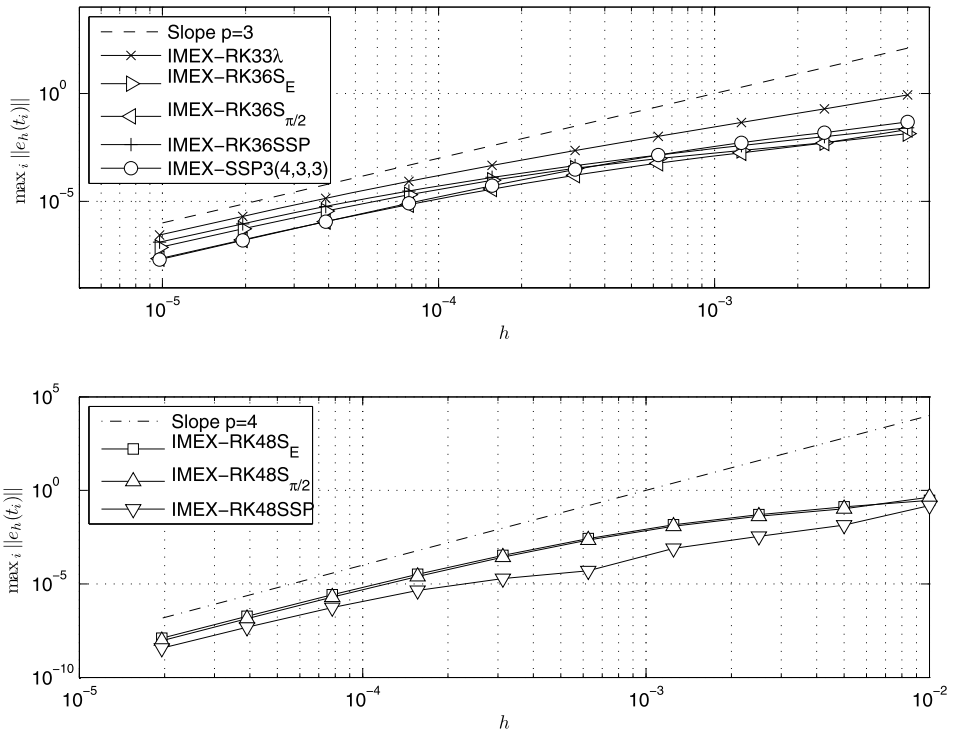

Fig. 6.5. Error versus stepsize (double logarithmic scale plot) for IMEX RK methods of order $p = 3$ and $p = 4$ on the one-dimensional shallow water problem (6.5) with boundary conditions (6.6) and $\varepsilon = 10^{-4}$.

Even if the order reduction phenomenon can occur for large values of the stepsize, numerical examples illustrate that the methods derived in this paper perform well for some range of the stepsize on stiff differential systems arising in different fields of applications, such as the semi-discretization in space variables of time dependent PDEs.

Future work will address the construction of IMEX GLMs of high order and stage order with inherent Runge–Kutta stability, which do not suffer from order reduction phenomenon.

Acknowledgements

The results reported in this paper were obtained during the visit of the first author (GI) to the Arizona State University in the Spring semester of 2014. This author wish to express his gratitude to the School of Mathematical & Statistical Sciences for hospitality during this visit.

References

[1] U.M. Asher, S.J. Ruuth, R.J. Spiteri, Implicit–explicit Runge–Kutta methods for time-dependent partial differential equations, Appl. Numer. Math. 25 (1997) 151–167.
[2] U.M. Asher, S.J. Ruuth, B. Wetton, Implicit-explicit methods for time dependent PDE's, SIAM J. Numer. Anal. 32 (1995) 797–823.
[3] Z. Bartoszewski, Z. Jackiewicz, Explicit Nordsieck methods with extended stability regions, Appl. Math. Comput. 218 (2012) 6056–6066.
[4] S. Boscarino, Error analysis of IMEX Runge–Kutta methods derived from differential-algebraic systems, SIAM J. Numer. Anal. 45 (2007) 1600–1621.
[5] S. Boscarino, On the accurate third order implicit–explicit Runge–Kutta methods for stiff problems, Appl. Numer. Math. 59 (2009) 1515–1528; 37 (2015), B305–B331.
[6] S. Boscarino, R. Bürger, P. Mulet, G. Russo, M.L. Villada, Linearly implicit IMEX Runge–Kutta methods for a class of degenerate convection–diffusion problems, SIAM J. Sci. Comput. 37 (2) (2015) B305–B331.
[7] S. Boscarino, G. Russo, On a class of uniformly accurate IMEX Runge–Kutta schemes and applications to hyperbolic systems with relaxation, SIAM J. Sci. Comput. 31 (2009) 1926–1945.
[8] M. Braś, G. Izzo, Z. Jackiewicz, Implicit-explicit general linear methods with inherent Runge–Kutta stability, J. Sci. Comput. (2016), http://dx.doi.org/10.1007/s10915-016-0273-y.
[9] J.C. Butcher, Numerical Methods for Ordinary Differential Equations, second edition, John Wiley & Sons, Chichester, 2008.
[10] A. Cardone, Z. Jackiewicz, A. Sandu, H. Zhang, Extrapolation-based implicit–explicit general linear methods, Numer. Algorithms 65 (2014) 377–399.
[11] A. Cardone, Z. Jackiewicz, A. Sandu, H. Zhang, Extrapolated implicit–explicit Runge–Kutta methods, Math. Model. Anal. 19 (2014) 18–43.
[12] A. Cardone, Z. Jackiewicz, A. Sandu, H. Zhang, Construction of highly stable implicit–explicit methods, Discrete Contin. Dyn. Syst., Ser. S 2015 (2015) 185–194.
[13] S. Gottlieb, D.I. Ketcheson, Chi-Wang Shu, Strong Stability Preserving Runge–Kutta and Multistep Time Discretizations, World Scientific Publishing Co. Pte. Ltd., Hackensack, NJ, 2011.
[14] S. Gottlieb, Chi-Wang Shu, E. Tadmor, Strong stability-preserving high-order time discretization methods, SIAM Rev. 43 (2001) 89–112.

[15] E. Hairer, G. Wanner, Solving Ordinary Differential Equations II, Stiff and Differential-Algebraic Problems, second revised edition, Springer-Verlag, Berlin, Heidelberg, New York, 1996.
[16] W. Hunndsdorfer, J.G. Verwer, Numerical Solution of Time-Dependent Advection-Diffusion-Reaction Equations, Springer-Verlag, Berlin, Heidelberg, New York, 2003.
[17] G. Izzo, Z. Jackiewicz, Construction of Strong Stability Preserving General Linear Methods, AIP Conference Proceedings, vol. 1648, 2015.
[18] G. Izzo, Z. Jackiewicz, Strong stability preserving general linear methods, J. Sci. Comput. 65 (1) (2014) 271–298.
[19] G. Izzo, Z. Jackiewicz, Strong stability preserving multistage integration methods, Math. Model. Anal. 20 (5) (2015) 552–577.
[20] Z. Jackiewicz, General Linear Methods for Ordinary Differential Equations, John Wiley, Hoboken, New Jersey, 2009.
[21] Z. Jackiewicz, S. Tracogna, A general class of two-step Runge–Kutta methods for ordinary differential equations, SIAM J. Numer. Anal. 32 (1995) 1390–1427.
[22] S. Jin, Runge–Kutta methods for hyperbolic systems with stiff relaxation terms, J. Comput. Phys. 122 (1995) 51–67.
[23] C.A. Kennedy, M.H. Carpenter, Additive Runge–Kutta schemes for convection–diffusion–reaction equations, Report NASA/TM-2001-211038, Langley Research Center, Hampton, Virginia, 2001.
[24] C.A. Kennedy, M.H. Carpenter, Additive Runge–Kutta schemes for convection–diffusion–reaction equations, Appl. Numer. Math. 44 (2003) 139–181.
[25] D.I. Ketcheson, S. Gottlieb, C.B. Macdonald, Strong stability preserving two-step Runge–Kutta methods, SIAM J. Numer. Anal. 49 (2011) 2618–2639.
[26] L. Pareschi, G. Russo, Implicit–explicit Runge–Kutta schemes for stiff systems of differential equations, in: Recent Trends in Numerical Analysis, in: Adv. Theory Comput. Math., vol. 3, Nova Sci. Publ., Huntington, NY, 2001, pp. 269–288.
[27] L. Pareschi, G. Russo, Implicit–explicit Runge–Kutta schemes and applications to hyperbolic systems with relaxation, J. Sci. Comput. 25 (2005) 129–155.
[28] J.E. Pearson, Complex patterns in a simple systems, Science 261 (1993) 189–192.
[29] J. Schnakenberg, Simple chemical reaction systems with limiting cycle behaviour, J. Theor. Biol. 81 (1979) 389–400.
[30] C.-W. Shu, High order ENO and WENO schemes for computational fluid dynamics, in: T.J. Barth, H. Deconinck (Eds.), High-Order Methods for Computational Physics, in: Lecture Notes in Computational Science and Engineering, vol. 9, Springer, 1999, pp. 439–582.
[31] M.N. Spijker, Stepsize conditions for general monotonicity in numerical initial value problems, SIAM J. Numer. Anal. 45 (2007) 1226–1245.
[32] H. Zhang, A. Sandu, A second-order diagonally-implicit multi-stage integration method, Proc. Comput. Sci. 9 (2012) 1039–1046.
[33] H. Zhang, A. Sandu, S. Blaise, Partitioned and implicit–explicit general linear methods for ordinary differential equations, J. Sci. Comput. 61 (2014) 119–144.
[34] E. Zharovsky, A. Sandu, H. Zhang, A class of implicit–explicit two-step Runge–Kutta methods, SIAM J. Numer. Anal. 53 (2015) 321–341.